

Projected Newton method for noise constrained ℓ_p regularization

J Cornelis & W Vanroose

Applied Mathematics Group, Department of Mathematics, University of Antwerp,
Middelheimlaan 1, 2020 Antwerp, Belgium

E-mail: jeffrey.cornelis@uantwerp.be

17 May 2022

Abstract. Choosing an appropriate regularization term is necessary to obtain a meaningful solution to an ill-posed linear inverse problem contaminated with measurement errors or noise. A regularization term in the ℓ_p norm with $p \geq 1$ covers a wide range of choices since its behavior critically depends on the choice of p and since it can easily be combined with a suitable regularization matrix. We develop an efficient algorithm that simultaneously determines the regularization parameter and corresponding ℓ_p regularized solution such that the discrepancy principle is satisfied. We project the problem on a low-dimensional Generalized Krylov subspace and compute the Newton direction for this much smaller problem. We illustrate some interesting properties of the algorithm and compare its performance with other state-of-the-art approaches using a number of numerical experiments, with a special focus of the sparsity inducing ℓ_1 norm and edge-preserving total variation regularization.

Keywords: Newton’s method, Generalized Krylov subspace, ℓ_p regularization, discrepancy principle, total variation

1. Introduction

In this manuscript we are concerned with the ℓ_p regularized linear inverse problem

$$x_\alpha = \operatorname{argmin}_{x \in \mathbb{R}^n} \frac{1}{2} \|Ax - b\|_2^2 + \frac{\alpha}{p} \|Lx\|_p^p \quad (1)$$

for $1 \leq p \leq 2$, where $A \in \mathbb{R}^{m \times n}$ is an ill-conditioned matrix that describes a forward operation, for example, modeling some physical process, and the data $b \in \mathbb{R}^m$ contains measurement errors or “noise”, such that $b = b_{ex} + e$. Without loss of generality we can assume that the “exact data” satisfies $b_{ex} = Ax_{ex}$ for some “exact solution” x_{ex} . It is well known that for such problems it is necessary to include a regularization term, since the naive solution (i.e. with $\alpha = 0$) is dominated by noise and does not provide any useful information about x_{ex} , see for instance [1]. The norm $\|x\|_p = (\sum_{i=1}^n |x_i|^p)^{\frac{1}{p}}$

denotes the standard ℓ_p norm of a vector $x \in \mathbb{R}^n$. For $p = 2$ we get the standard Euclidean norm and we sometimes use the simplified notation $\|x\|_2 = \|x\|$. The matrix $L \in \mathbb{R}^{s \times n}$ is referred to as the regularization matrix and is not necessarily square or invertible. It can be used to significantly improve the quality of the reconstruction. Regularization refers to the fact that we incorporate some prior knowledge about the exact solution x_{ex} to obtain a well-posed problem. For instance, if we know that the exact solution is smooth, then a good choice is standard form Tikhonov regularization, which corresponds to choosing $L = I_n$ the identity matrix of size n and $p = 2$. When we know that a certain transformation of x_{ex} is smooth, we can take $p = 2$ and choose a suitable regularization matrix $L \neq I_n$, in which case we refer to (1) as general form Tikhonov regularization. A popular choice of regularization matrix is, for instance, a finite-difference approximation of the first or second derivative operator. A wide range of efficient algorithms have been developed for the standard form and general form Tikhonov problem [2, 3, 4, 5].

The choice $L = I_n$ and $p = 1$ has also received a lot of attention in literature, since it is known that the ℓ_1 norm induces sparsity in the solution [6, 7, 8, 9, 10]. Total variation regularization [11, 12], which is a popular regularization technique in image deblurring, provides us of an example with $L \neq I_n$ and $p = 1$. Here the solution $x \in \mathbb{R}^n$ is a vector obtained by stacking all columns of a pixel image $X \in \mathbb{R}^{N \times N}$ with $n = N^2$ and the matrix A is a blurring operator. Let us denote the anisotropic total variation function as

$$\text{TV}(x) = \sum_{i,j=1}^N |\partial_h^{(i,j)}(X)| + |\partial_v^{(i,j)}(X)|. \quad (2)$$

with finite difference operators in the horizontal and vertical direction given by

$$\partial_h^{(i,j)}(X) = \begin{cases} X_{i,j+1} - X_{i,j} & j < N \\ 0 & j = N \end{cases} \quad \text{and} \quad \partial_v^{(i,j)}(X) = \begin{cases} X_{i+1,j} - X_{i,j} & i < N \\ 0 & i = N \end{cases}.$$

We can rewrite this in a more convenient way by first writing

$$D = \begin{pmatrix} 1 & -1 & & \\ & \ddots & \ddots & \\ & & 1 & -1 \end{pmatrix} \in \mathbb{R}^{(N-1) \times N} \quad (3)$$

which represents a finite difference approximation of the derivative operator in one dimension. Let \otimes denote the kronecker product. We can compactly write $\text{TV}(x) = \|Lx\|_1$ with

$$L = \begin{pmatrix} D_h \\ D_v \end{pmatrix} \in \mathbb{R}^{(2n-2N) \times n} \quad \text{and} \quad \begin{cases} D_h = D \otimes I_N \in \mathbb{R}^{(n-N) \times n} \\ D_v = I_N \otimes D \in \mathbb{R}^{(n-N) \times n} \end{cases}. \quad (4)$$

The matrices D_h and D_v represent the two dimensional finite difference approximation in the horizontal and the vertical direction respectively.

The scalar $\alpha \in \mathbb{R}$ in (1) is called the regularization parameter and has a huge impact on the quality of the reconstruction. If we choose this value too small, then the solution x_α closely resembles the naive solution, which we know is “over-fitted” to the noisy data b . On the other hand, if we choose α too large, then x_α is not a good solution to the inverse problem anymore and is, for instance, in the case of Tikhonov regularization “over-smoothed”. Different parameter choice methods exist for choosing a suitable α . One of the most straightforward ways to choose the regularization parameter is given by the discrepancy principle, which states that we should choose α such that

$$\|Ax_\alpha - b\|_2 = \eta \|e\|_2 \quad (5)$$

where $\eta \geq 1$ is a safety factor. Obviously $\|e\|_2$ is not available in practice, so this approach assumes we have some estimate of this value available.

Note that (1) is a convex optimization problem, which means that any local solution is also a global solution. However, for $p < 2$ the problem is non-differentiable. Hence, we cannot use algorithms that rely on the gradient or Hessian of the objective function, like steepest descent or Newton’s method [13]. To overcome this issue, we simply use a smooth approximation of the regularization term $\|Lx\|_p^p$ when $p < 2$.

In this paper we develop an algorithm that simultaneously solves (a smooth approximation of) the ℓ_p regularized problem (1) and determines the corresponding regularization parameter α such that the discrepancy principle (5) is satisfied. This problem can be reformulated as a constrained optimization problem for which the solution satisfies a system of nonlinear equations. Newton’s method can be used to solve this problem [14].

However, this approach can be quite computationally expensive for large-scale problems since each iteration requires the solution of a large linear system to obtain the Newton direction. A Krylov subspace method is typically used to solve the linear system, leading to an expensive outer-inner iteration scheme, i.e. each outer Newton iteration requires a number of inner Krylov subspace iterations. We circumvent this by projecting the constrained optimization problem on a low-dimensional Generalized Krylov subspace and calculating the Newton direction for this projected problem. In each iteration of the algorithm we use this search direction in combination with a backtracking line search, after which the Generalized Krylov subspace is expanded. Further improvements to the algorithm are presented in the case of general form Tikhonov regularization. This newly developed algorithm can be seen as a generalization of the Projected Newton method for standard form Tikhonov regularization [3]. In fact, some results from [3] are extended and proven in a more general context.

The paper is organized as follows. In section 2 we define a smooth approximation of the ℓ_p norm and provide some intuition by looking at the optimality condition of the ℓ_1 regularized problem. In section 3, we formulate the nonlinear system of equations that describes the problem of interest. The main contribution of this paper is presented in section 4, where we develop the Projected Newton method and prove our main results. Section 5 describes two reference methods that we use to compare the Projected Newton

method with. Next, in section 6 we provide a number of experiments illustrating the performance and overall behavior of the newly proposed algorithm. Lastly, this work is concluded in section 7.

2. Smooth approximation of the ℓ_p norm

The ℓ_p norm is non-differentiable for $p < 2$, which makes the optimization problem a bit more difficult. However, it is easy to formulate a smooth approximation $\Psi_p(x) \approx \frac{1}{p} \|x\|_p^p$ where $\Psi_p : \mathbb{R}^n \rightarrow \mathbb{R}$ is a twice continuously differentiable convex function, more precisely we define

$$\Psi_p(x) = \frac{1}{p} \sum_{i=1}^n (x_i^2 + \beta)^{\frac{p}{2}} \quad (6)$$

where $\beta > 0$ is a small scalar that ensures smoothness. Other possible smooth approximations of the absolute value function can alternatively be chosen. The gradient $\nabla \Psi_p(x) = \left(\frac{\partial \Psi_p(x)}{\partial x_1}, \dots, \frac{\partial \Psi_p(x)}{\partial x_n} \right)^T$ is given by the partial derivatives

$$\frac{\partial \Psi_p(x)}{\partial x_i} = x_i (x_i^2 + \beta)^{\frac{p}{2}-1}$$

for $i = 1, \dots, n$. The Hessian matrix $\nabla^2 \Psi_p(x) = \left(\frac{\partial^2 \Psi_p(x)}{\partial x_i \partial x_j} \right)_{i,j=1,\dots,n}$ is a diagonal matrix since $\frac{\partial \Psi_p(x)}{\partial x_i}$ does not contain any x_j with $i \neq j$ and is thus given by the following second derivatives:

$$\frac{\partial^2 \Psi_p(x)}{\partial x_i^2} = (x_i^2 + \beta)^{\frac{p}{2}-1} + 2\left(\frac{p}{2} - 1\right) x_i^2 (x_i^2 + \beta)^{\frac{p}{2}-2} > 0.$$

From this it also follows that $\Psi_p(x)$ is strictly convex. The following lemma can be used to calculate the gradient and Hessian for the smooth approximation $\Psi_p(Lx) \approx \frac{1}{p} \|Lx\|_p^p$.

Lemma 2.1. *Let $L \in \mathbb{R}^{s \times n}$ and $x \in \mathbb{R}^n$. Let $\tilde{\Psi}(z) : \mathbb{R}^s \rightarrow \mathbb{R}$ be a twice continuously differentiable function and $\Psi(x) = \tilde{\Psi}(Lx)$, then we have*

$$\begin{aligned} \nabla \Psi(x) &= L^T \nabla \tilde{\Psi}(Lx), \\ \nabla^2 \Psi(x) &= L^T \nabla^2 \tilde{\Psi}(Lx) L. \end{aligned}$$

Proof. This follows from the chain rule for multivariate functions. \square

The smooth approximation $\Psi_p(x)$ has an interesting interpretation if we look at the optimality condition of the minimization of a non-differentiable function. Let us consider the example with $L = I_n$ and $p = 1$:

$$\min_{x \in \mathbb{R}^n} \frac{1}{2} \|Ax - b\|_2^2 + \alpha \|x\|_1. \quad (7)$$

Optimality can be expressed using the sub-differential $\partial \|x\|_1$, which is the set of all sub-gradients g of $\|x\|_1$. In general, $g \in \mathbb{R}^n$ is a sub-gradient of a convex function $f : \mathbb{R}^n \rightarrow \mathbb{R}$ in a point $x \in \mathbb{R}^n$ if and only if $\forall y \in \mathbb{R}^n$ we have

$$f(y) \geq f(x) + g^T(y - x).$$

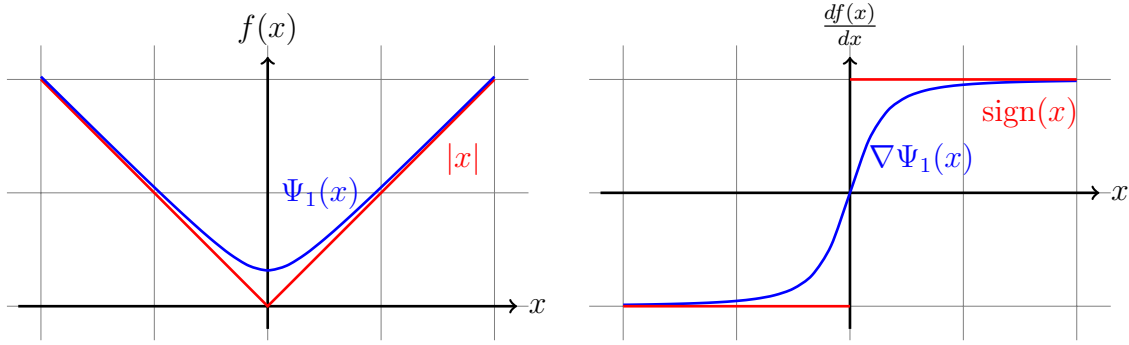


Figure 1: Illustration of the smooth approximation $\Psi_1(x)$ of $|x|$ (left) and respective derivative $\nabla\Psi_1(x)$ and $\text{sign}(x)$ (right) for $x \in \mathbb{R}$ with $\beta = 0.1$.

When f is differentiable in x , the sub-gradient in x is unique and coincides with the usual gradient, i.e. we have that $\partial f(x) = \{\nabla f(x)\}$, see for instance [15]. The sub-gradient of the absolute value function (in one dimension) for $x \neq 0$ is $\partial|x| = \{\text{sign}(x)\}$, while for $x = 0$ the sub-gradient has to satisfy the inequality $|y| \geq gy$ which is satisfied if and only if $g \in [-1, 1]$, i.e. $\partial|0| = [-1, 1]$.

We can now write that x solves the minimization problem (7) if and only if

$$0 \in A^T(Ax - b) + \alpha \partial\|x\|_1,$$

where an element $g \in \partial\|x\|_1$ has component $g_i = \text{sign}(x_i)$ when the i th component of x_i is nonzero and $g_i \in [-1, 1]$ for $x_i = 0$. The smooth approximation for $\|x\|_1$ is $\Psi_1(x) = \sum_{i=1}^n \sqrt{x_i^2 + \beta}$ with gradient and Hessian respectively given by

$$\nabla\Psi_1(x) = \frac{x}{\sqrt{x^2 + \beta}} \quad \text{and} \quad \nabla^2\Psi_1(x) = \text{diag}\left(\frac{\beta}{(x^2 + \beta)^{3/2}}\right) \quad (8)$$

where the division should be interpreted component-wise. When β is very small we have that $\nabla\Psi_1(x)$ is a good approximation of the sign function $\text{sign}(x)$. Hence, same as $\Psi_1(x)$ is a smooth approximation of $\|x\|_1$, we have that the gradient $\nabla\Psi_1(x)$ can be interpreted as a smooth approximation of $\partial\|x\|_1$. See figure 1 for an illustration in one dimension.

3. Reformulation of the problem

For the moment, let us denote $\Psi(x) : \mathbb{R}^n \rightarrow \mathbb{R}$ any twice continuously differentiable convex function. For instance, for the smooth approximation of the regularization term $\frac{1}{p}\|Lx\|_p^p$ with $1 \leq p < 2$ we take $\Psi(x) = \Psi_p(Lx)$, while for $p = 2$ we simply take the actual regularization term $\frac{1}{2}\|Lx\|_2^2$ since it is already smooth. The goal is to develop an efficient algorithm that can simultaneously solve the convex optimization problem

$$x_\alpha = \underset{x \in \mathbb{R}^n}{\text{argmin}} \frac{1}{2}\|Ax - b\|_2^2 + \alpha\Psi(x), \quad (9)$$

and find the corresponding regularization parameter α such that the discrepancy principle (5) is satisfied. Note that this goal is slightly more general than expressed in the introduction. The (possibly nonlinear) system of equations

$$A^T(Ax - b) + \alpha \nabla \Psi(x) = 0 \quad (10)$$

are necessary and sufficient conditions for x to be a global solution for (9) due to convexity of the objective function. Uniqueness of the solution is in general not guaranteed. For instance, if we want to ensure a unique solution for general form Tikhonov regularization we need to add the requirement that $\mathcal{N}(A) \cap \mathcal{N}(L) = \{0\}$, where $\mathcal{N}(\cdot)$ denotes the null-space of a matrix. In fact, the following more general result holds

Lemma 3.1. *Let $\Psi(x) = \tilde{\Psi}(Lx)$ with a twice continuously differentiable strictly convex function $\tilde{\Psi}(z) : \mathbb{R}^s \rightarrow \mathbb{R}$ and $L \in \mathbb{R}^{s \times n}$ such that $\mathcal{N}(A) \cap \mathcal{N}(L) = \{0\}$ then it holds that (9) has a unique solution.*

Proof. Let x_1 and x_2 be two different solutions. It is not possible that both $Lx_1 = Lx_2$ and $Ax_1 = Ax_2$ since this would imply $x_1 - x_2 \in \mathcal{N}(A) \cap \mathcal{N}(L)$. Let us denote $x_3 = (x_1 + x_2)/2$. Suppose $Lx_1 \neq Lx_2$, then we have that $\tilde{\Psi}(Lx_3) < \frac{1}{2}\tilde{\Psi}(Lx_1) + \frac{1}{2}\tilde{\Psi}(Lx_2)$ since $\tilde{\Psi}$ is strictly convex. If $Lx_1 = Lx_2$ then we must have $Ax_1 \neq Ax_2$ and we have in this case $\|Ax_3 - b\|^2 < \frac{1}{2}\|Ax_1 - b\|^2 + \frac{1}{2}\|Ax_2 - b\|^2$ since the squared Euclidean norm is also strictly convex. Hence, at least one of these inequalities is strict. This implies that

$$\frac{1}{2}\|Ax_3 - b\|_2^2 + \alpha \tilde{\Psi}(Lx_3) < \frac{1}{4}\|Ax_1 - b\|_2^2 + \frac{\alpha}{2}\tilde{\Psi}(Lx_1) + \frac{1}{4}\|Ax_2 - b\|_2^2 + \frac{\alpha}{2}\tilde{\Psi}(Lx_2)$$

This leads to a contradiction since every local solution is a global solution and we have found a point x_3 with strictly smaller objective value than x_1 and x_2 . \square

Recall that $\tilde{\Psi}(z) = \Psi_p(z)$ is strictly convex and thus it follows from this lemma that the smooth approximation of the ℓ_p regularized problem has a unique solution if $\mathcal{N}(A) \cap \mathcal{N}(L) = \{0\}$.

Let us consider the following closely related constrained optimization problem

$$\min_{x \in \mathbb{R}^n} \Psi(x) \quad \text{subject to} \quad \frac{1}{2}\|Ax - b\|_2^2 = \frac{\sigma^2}{2} \quad (11)$$

where we denote $\sigma = \eta\|e\|_2$ the value used in the discrepancy principle (5). A solution (x^*, λ^*) to (11) has to satisfy the nonlinear system of equations $F(x^*, \lambda^*) = 0$ with

$$F(x, \lambda) = \begin{pmatrix} \lambda A^T(Ax - b) + \nabla \Psi(x) \\ \frac{1}{2}\|Ax - b\|_2^2 - \frac{\sigma^2}{2} \end{pmatrix} \in \mathbb{R}^{n+1}. \quad (12)$$

These express the first order optimality conditions, also known as Karush-Kuhn-Tucker or KKT-conditions [13]. The author in [14] showed, under some mild technical

assumption[‡], that they are sufficient conditions for (x^*, λ^*) to be a global solution and that the Lagrange multiplier λ is strictly positive. Now, if (x, λ) is any root of the first component of (12) with $\lambda > 0$ it is also a solution to (9) for $\alpha = 1/\lambda$, which follows from the fact that (x, α) solves the optimality conditions (10) in that case. This means that if we solve (11) we simultaneously solve the regularized linear inverse problem (9) and find the corresponding regularization parameter ($\alpha = 1/\lambda$) such that the discrepancy principle is satisfied. Due to the straightforward connection between α and λ we refer to both quantities as the regularization parameter. Uniqueness of the solution of (11) can be proven under the same conditions as lemma 3.1 using similar arguments as presented in its proof.

The Newton direction for the nonlinear system of equations $F(x, \lambda) = 0$ in a point (x, λ) is given by the solution of the linear system

$$J(x, \lambda) \begin{pmatrix} \Delta x \\ \Delta \lambda \end{pmatrix} = -F(x, \lambda) \quad (13)$$

where the Jacobian $J(x, \lambda) \in \mathbb{R}^{(n+1) \times (n+1)}$ of the function $F(x, \lambda)$ is given by

$$J(x, \lambda) = \begin{pmatrix} \lambda A^T A + \nabla^2 \Psi(x) & A^T (Ax - b) \\ (Ax - b)^T A & 0 \end{pmatrix}. \quad (14)$$

This linear system (13) can not be solved using a direct method when n is very large. Moreover, for many applications the matrix A is not explicitly given and we can only compute matrix-vector products with A and A^T . Hence, a Krylov subspace method such as MINRES [16] is used to compute the Newton direction. However, every iteration of the linear solver requires a matrix-vector product with A and A^T , which becomes expensive when a lot of iterations need to be performed.

4. Projected Newton method

In this section we derive a Newton-type method that solves (11) and that only requires one matrix-vector product with A and one matrix-vector product with A^T in each iteration.

4.1. Projected minimization problem

Suppose we have a matrix $V_k = [v_0, v_1, \dots, v_{k-1}] \in \mathbb{R}^{n \times k}$ with orthonormal columns, i.e. $V_k^T V_k = I_k$. The index k is the iteration index of the algorithm that we describe in this section. Here and in what follows a sub-index refers to a certain iteration number rather than, for instance, an element of a vector. Let $\mathcal{R}(V_k)$ denote the range of the matrix

[‡] The assumption being that there exists a constant $c \geq 0$ such that for all x it holds that $\Psi(x) \geq c$, $\Psi(0) = c$ and that $\{x : \Psi(x) = c\} \cap \{x : \|Ax - b\| \leq \sigma\} = \emptyset$.

V_k , i.e. the space spanned by all columns of the matrix. We consider the k -dimensional *projected minimization problem*

$$\begin{aligned} \min_{x \in \mathcal{R}(V_k)} \Psi(x) \quad & \text{subject to} \quad \frac{1}{2} \|Ax - b\|_2^2 = \frac{\sigma^2}{2} \\ \Leftrightarrow \min_{y \in \mathbb{R}^k} \Psi(V_k y) \quad & \text{subject to} \quad \frac{1}{2} \|AV_k y - b\|_2^2 = \frac{\sigma^2}{2}. \end{aligned} \quad (15)$$

The corresponding equation for the KKT conditions is now given by

$$F^{(k)}(y, \lambda) = \begin{pmatrix} \lambda V_k^T A^T (AV_k y - b) + V_k^T \nabla \Psi(V_k y) \\ \frac{1}{2} \|AV_k y - b\|_2^2 - \frac{\sigma^2}{2} \end{pmatrix} = \begin{pmatrix} V_k^T & 0 \\ 0 & 1 \end{pmatrix} F(V_k y, \lambda) \quad (16)$$

which can be seen as a projected version of (12). The Jacobian of the *projected function* $F^{(k)}(y, \lambda) \in \mathbb{R}^{k+1}$, which we refer to as the *projected Jacobian*, is given by

$$J^{(k)}(y, \lambda) = \begin{pmatrix} \lambda V_k^T A^T AV_k + V_k^T \nabla^2 \Psi(V_k y) V_k & V_k^T A^T (AV_k y - b) \\ (AV_k y - b)^T AV_k & 0 \end{pmatrix} \in \mathbb{R}^{(k+1) \times (k+1)}. \quad (17)$$

We have the following connection between the Jacobian (14) and projected Jacobian

$$J^{(k)}(y, \lambda) = \begin{pmatrix} V_k^T & 0 \\ 0 & 1 \end{pmatrix} J(V_k y, \lambda) \begin{pmatrix} V_k & 0 \\ 0 & 1 \end{pmatrix}. \quad (18)$$

Let us denote $\bar{y}_{k-1} = (y_{k-1}^T, 0)^T \in \mathbb{R}^k$ for $k > 1$ where y_{k-1} is an approximate solution for the $(k-1)$ -dimensional minimization problem and $\bar{y}_0 = 0$. Let us furthermore write $x_k = V_k y_k$ for all $k > 0$ and $x_0 = 0$. Since the last component of \bar{y}_{k-1} is zero we have $V_k \bar{y}_{k-1} = V_{k-1} y_{k-1} = x_{k-1}$ for $k > 1$ and $V_1 \bar{y}_0 = x_0 = 0$ by definition. If $J^{(k)}(\bar{y}_{k-1}, \lambda_{k-1})$ is nonsingular we can calculate the Newton direction for the projected problem as the solution of the linear system

$$J^{(k)}(\bar{y}_{k-1}, \lambda_{k-1}) \begin{pmatrix} \Delta y_k \\ \Delta \lambda_k \end{pmatrix} = -F^{(k)}(\bar{y}_{k-1}, \lambda_{k-1}) \quad (19)$$

and we refer to this as the *projected Newton direction*. For a suitably chosen step-length $0 < \gamma_k \leq 1$, we can update our sequence by

$$y_k = \bar{y}_{k-1} + \gamma_k \Delta y_k, \quad \lambda_k = \lambda_{k-1} + \gamma_k \Delta \lambda_k.$$

This gives us a corresponding update for x_k :

$$x_k = V_k y_k = V_k \bar{y}_{k-1} + \gamma_k V_k \Delta y_k = x_{k-1} + \gamma_k \Delta x_k,$$

where we define $\Delta x_k = V_k \Delta y_k$. Note that this step is different from the step that would be obtained by calculating the true Newton direction $J(x_{k-1}, \lambda_{k-1})^{-1} F(x_{k-1}, \lambda_{k-1})$. However, if we choose a particular basis V_k , we will show that this provides us with a descent direction for the merit function $f(x, \lambda) = \frac{1}{2} \|F(x, \lambda)\|^2$.

In general we can not conclude from (16) that

$$\begin{pmatrix} V_k & 0 \\ 0 & 1 \end{pmatrix} F^{(k)}(\bar{y}_{k-1}, \lambda_{k-1}) = F(V_k \bar{y}_{k-1}, \lambda_{k-1}). \quad (20)$$

However, by considering a specific choice of basis V_k we can enforce this equality. Recall that $V_k \bar{y}_{k-1} = x_{k-1}$. Let us denote

$$\tilde{v}_{k-1} = \lambda_{k-1} A^T (Ax_{k-1} - b) + \nabla \Psi(x_{k-1}) \quad (21)$$

the first component of $F(x_{k-1}, \lambda_{k-1})$, see (12). Equation (20) holds if and only if

$$V_k V_k^T \tilde{v}_{k-1} = \tilde{v}_{k-1}$$

which is true if $\tilde{v}_{k-1} \in \mathcal{R}(V_k)$. Now we have a straightforward way to construct the basis $V_k = [v_0, \dots, v_{k-1}]$ such that (20) holds. Let $V_1 = \tilde{v}_0 / \|\tilde{v}_0\|$. Suppose we already have the basis V_k in iteration k and have just constructed new variables λ_k and x_k . To add a new vector v_k to get V_{k+1} , we simply take \tilde{v}_k and orthogonalize it to all previous vectors in V_k using Gram-Schmidt and then normalize, i.e:

$$v_k = \tilde{v}_k - \sum_{j=0}^{k-1} (v_j^T \tilde{v}_k) v_j, \quad v_k = v_k / \|v_k\|. \quad (22)$$

Note that we use modified Gram-Schmidt in the actual implementation of the algorithm, but for notational convenience we write in the classical way. By construction we now have that V_k has orthonormal columns and

$$\mathcal{R}(V_{k+1}) = \text{span} \{ \tilde{v}_0, \tilde{v}_1, \dots, \tilde{v}_k \}. \quad (23)$$

The basis V_k is unique up to sign change of each of the vectors. First note that when the k -dimensional projected minimization problem (15) is solved for $y = y_k$, which does not necessarily imply that the original problem is solved, we have that $\lambda_k V_k^T A^T (Ax_k - b) + V_k^T \nabla \Psi(x_k) = 0$. This implies that \tilde{v}_k is already orthogonal to V_k and then the Gram-Schmidt procedure is in principle not necessary. In this case (22) can be seen as a reorthogonalization step.

Secondly, we note that the basis V_k can be seen as a Generalized Krylov subspace, similarly as in [4]. Indeed, let us denote the Krylov subspace of dimension k for $M \in \mathbb{R}^{n \times n}$ and $v \in \mathbb{R}^n$ as $\mathcal{K}_k(M, v) = \text{span} \{ v, Mv, \dots, M^{k-1}v \}$. Consider the case when $\Psi(x) = \frac{1}{2} \|x\|^2$, i.e. standard form Tikhonov regularization. Then we have

$$\tilde{v}_{k-1} = \lambda_{k-1} A^T (Ax_{k-1} - b) + x_{k-1} = (\lambda_{k-1} A^T A + I_n) x_{k-1} - A^T b$$

In particular for $x_0 = 0$ we have $v_0 = \pm A^T b / \|A^T b\|$. Now, due to the shift invariance of Krylov subspaces, i.e. the fact that

$$\mathcal{K}_k(A^T A, A^T b) = \mathcal{K}_k(A^T A + \alpha I, A^T b), \quad \forall \alpha \in \mathbb{R} \quad (24)$$

it can easily be seen that $\mathcal{R}(V_k) = \mathcal{K}_k(A^T A, A^T b)$. As a consequence, we now also have that $V_k^T A^T A V_k$ is a tridiagonal matrix. This is because the basis V_k is (up to sign change of the vectors) the same basis as generated by the Golub-Kahan bidiagonalization procedure [17, 18]. This basis satisfies a relation of the form $AV_k = U_{k+1}B_{k+1,k}$ with an upper bidiagonal matrix $B_{k+1,k} \in \mathbb{R}^{(k+1) \times k}$ and matrix $U_{k+1} \in \mathbb{R}^{m \times n}$ with orthonormal columns. Hence, we get $V_k^T A^T A V_k = B_{k+1,k}^T B_{k+1,k}$, which is indeed tridiagonal. Note that the Golub-Kahan bidiagonalization procedure is used in the Projected Newton method for standard form Tikhonov regularization [3]. Hence, the results presented in this section can be seen as a generalization of some of the results in [3]. In fact, the algorithm presented in the current paper, when applied to the standard form Tikhonov problem, is (in exact arithmetic) equivalent to the algorithm presented in [3], although implemented in a different way.

When we consider, for instance, general form Tikhonov regularization, i.e. $\Psi(x) = \frac{1}{2} \|Lx\|^2$ with $L \neq I_n$ we do not have in general that V_k spans a Krylov subspace. This would only be true if the regularization parameter λ_k remains the same for all k . The interesting thing to note, however, is that if the parameter λ_k stabilizes quickly, then we can recognize a kind of tridiagonal structure in $V_k^T (A^T A + \alpha_k L^T L) V_k$ with $\alpha_k = 1/\lambda_k$. More precisely the elements on the three main diagonals have much larger magnitude than all other elements. We illustrate this in a small numerical experiment in section 6.

Using the Generalized Krylov subspace basis V_k as described above, we can prove the following theorem:

Theorem 4.1. *Let V_k be the Generalized Krylov subspace basis (23) and $(\Delta y_k^T, \Delta \lambda_k)^T$ be the Projected Newton direction obtained by solving (19). Then the step $\Delta_k = (\Delta x_k^T, \Delta \lambda_k)^T$ with $\Delta x_k = V_k \Delta y_k$ is either a descent direction for $f(x_{k-1}, \lambda_{k-1})$, i.e.*

$$\Delta_k^T \nabla f(x_{k-1}, \lambda_{k-1}) < 0$$

or we have found a solution to (11).

Proof. Using (18), which holds for any matrix V_k , and (20), which holds for the Generalized Krylov subspace basis V_k , together with the definition of the step Δ_k we have:

$$\begin{aligned} \Delta_k^T \nabla f(x_{k-1}, \lambda_{k-1}) &= \begin{pmatrix} \Delta x_k \\ \Delta \lambda_k \end{pmatrix}^T J(x_{k-1}, \lambda_{k-1}) F(x_{k-1}, \lambda_{k-1}) \\ &= \begin{pmatrix} V_k \Delta y_k \\ \Delta \lambda_k \end{pmatrix}^T J(V_k \bar{y}_{k-1}, \lambda_{k-1}) F(V_k \bar{y}_{k-1}, \lambda_{k-1}) \\ &= \begin{pmatrix} \Delta y_k \\ \Delta \lambda_k \end{pmatrix}^T \begin{pmatrix} V_k^T & 0 \\ 0 & 1 \end{pmatrix} J(V_k \bar{y}_{k-1}, \lambda_{k-1}) \begin{pmatrix} V_k & 0 \\ 0 & 1 \end{pmatrix} F^{(k)}(\bar{y}_{k-1}, \lambda_{k-1}) \\ &= \begin{pmatrix} \Delta y_k \\ \Delta \lambda_k \end{pmatrix}^T J^{(k)}(\bar{y}_{k-1}, \lambda_{k-1}) F^{(k)}(\bar{y}_{k-1}, \lambda_{k-1}) \end{aligned}$$

$$\begin{aligned}
&= - \left(J^{(k)}(\bar{y}_{k-1}, \lambda_{k-1})^{-1} F^{(k)}(\bar{y}_{k-1}, \lambda_{k-1}) \right)^T J^{(k)}(\bar{y}_{k-1}, \lambda_{k-1}) F^{(k)}(\bar{y}_{k-1}, \lambda_{k-1}) \\
&= - \|F^{(k)}(\bar{y}_{k-1}, \lambda_{k-1})\|^2 = -\|F(x_{k-1}, \lambda_{k-1})\|^2 \leq 0.
\end{aligned}$$

The proof now follows from the fact that (x_{k-1}, λ_{k-1}) is a solution to (11) if and only if $\|F(x_{k-1}, \lambda_{k-1})\| = 0$. \square

The importance of the above theorem is illustrated by the fact that for γ_k small enough we have by Taylor's theorem [13, 19] that

$$f(x_{k-1} + \gamma_k \Delta x_k, \lambda_{k-1} + \gamma_k \Delta \lambda_k) \approx f(x_{k-1}, \lambda_{k-1}) + \gamma_k \Delta_k^T \nabla f(x_{k-1}, \lambda_{k-1})$$

which implies we can find a step-length γ_k such that we have a strict decrease in the merit function $f(x_k, \lambda_k) < f(x_{k-1}, \lambda_{k-1})$. In practice, a so-called backtracking line search is often used to find a step-length $\gamma_k > 0$ such that there is a “sufficient decrease” of the objective function:

$$\frac{1}{2} \|F(x_k, \lambda_k)\|^2 \leq \left(\frac{1}{2} - c\gamma_k \right) \|F(x_{k-1}, \lambda_{k-1})\|^2 \quad (25)$$

with $c \in (0, 1)$. Equation (25) is often referred to in literature as the sufficient decrease condition or Armijo condition. To find such a step-length, we simply start with $\gamma_k = 1$ and check if the sufficient decrease condition holds. If not, we reduce γ_k by a factor $0 < \tau < 1$ and check if $\gamma_k := \tau\gamma_k$, satisfies the condition. This procedure is then repeated until a suitable step-length is found. We obviously do not want to calculate the new norm $F(x_k, \lambda_k)$ by performing matrix-vector products with A and A^T . This would make the line search expensive if the step-length is reduced multiple times. In section 4.3 we describe how this line search can be performed efficiently.

For the sake of presentation, let us assume that $\nabla \Psi(0) = 0$, which is true for $\Psi(x) = \Psi_p(Lx)$ and $\Psi(x) = \frac{1}{2} \|Lx\|_2^2$. In that case we can choose $v_0 = A^T b / \|A^T b\|$. The basic idea of the proposed algorithm is the following:

- (i) Initialize $k = 1, x_0 = 0, V_1 = A^T b / \|A^T b\|$ and choose $\lambda_0 > 0$.
- (ii) Calculate descent direction $\Delta_k = (\Delta x_k^T, \Delta \lambda_k)^T$ with $\Delta x_k = V_k \Delta y_k$ using (19).
- (iii) Choose step-length γ_k such that sufficient decrease condition (25) is satisfied.
- (iv) Expand Generalized Krylov subspace basis $V_{k+1} = [V_k, v_k]$ using (21) and (22).
- (v) Increase iteration index $k = k + 1$.
- (vi) Repeat (ii)-(v) until convergence.

In section 6 we comment on the different criteria that can be used to check for convergence in step (vi). The following interesting result will be useful in this discussion.

Lemma 4.2. *For all $k \geq 0$ we have that the iterates x_k generated by steps (i)-(vi) outlined above satisfy $\|Ax_k - b\| \geq \sigma$, which means we never get a residual smaller than what the discrepancy principle dictates.*

Proof. We prove this by induction. For $k = 0$ we have trivially have $\|b\| \geq \sigma$, since otherwise the noise is larger than the data and there is no use in trying to solve the inverse problem. So suppose we have $k > 0$ and that $\|Ax_{k-1} - b\| = \|AV_k \bar{y}_{k-1} - b\| \geq \sigma$. Writing out the last component of the equality (19) we get

$$(AV_k \bar{y}_{k-1} - b)^T AV_k \Delta y_k = \frac{\sigma^2}{2} - \frac{1}{2} \|AV_k \bar{y}_{k-1} - b\|^2 \leq 0.$$

Now the proof follows from the following calculation

$$\begin{aligned} \|Ax_k - b\|^2 &= \|AV_k y_k - b\|^2 = \|AV_k(\bar{y}_{k-1} + \gamma_k \Delta y_k) - b\|^2 \\ &= \|AV_k \bar{y}_{k-1} - b\|^2 + \gamma_k^2 \|AV_k \Delta y_k\|^2 + 2\gamma_k (AV_k \bar{y}_{k-1} - b)^T AV_k \Delta y_k \\ &\geq \|AV_k \bar{y}_{k-1} - b\|^2 + \gamma_k^2 \|AV_k \Delta y_k\|^2 + 2(AV_k \bar{y}_{k-1} - b)^T AV_k \Delta y_k \\ &= \sigma^2 + \gamma_k^2 \|AV_k \Delta y_k\|^2. \end{aligned} \quad \square$$

4.2. Efficiently computing the projected Newton direction

In this section we efficiently construct the projected Jacobian (17) and projected function (16) that we need to compute the projected Newton direction (19). To do so, we consider the reduced QR decomposition of the tall and skinny matrix $AV_k \in \mathbb{R}^{m \times k}$, which was also the approach taken in [4, 20]. Let $Q_k \in \mathbb{R}^{m \times k}$ with $Q_k^T Q_k = I_k$ and $R_k \in \mathbb{R}^{k \times k}$ upper triangular such that $AV_k = Q_k R_k$. Using this QR decomposition we can write $V_k^T A^T AV_k = R_k^T R_k$ and as a consequence we also have

$$V_k^T A^T (AV_k y - b) = R_k^T R_k y - V_k^T A^T b = R_k^T R_k y - d_k \quad (26)$$

with $d_k = V_k^T A^T b = \|A^T b\| e_1^{(k)}$ and $e_1^{(k)} = (1, 0, \dots, 0)^T \in \mathbb{R}^k$. The vector (26) is present in both the projected Jacobian (17) and the projected function (16). The QR decomposition of AV_k can be efficiently updated in each iteration. For $k = 1$ we trivially have $AV_1 = Q_1 R_1$ with $R_1 = \|AV_1\|$ and $Q_1 = AV_1/R_1$. For $k > 1$ we can write

$$AV_k = [AV_{k-1}, Av_{k-1}] = [Q_{k-1} R_{k-1}, Av_{k-1}] = \underbrace{[Q_{k-1}, q_k]}_{:=Q_k} \underbrace{\begin{pmatrix} R_{k-1} & r_k \\ 0 & r_{k,k} \end{pmatrix}}_{:=R_k} \quad (27)$$

$$\text{with } r_k = Q_{k-1}^T Av_{k-1}, \quad \tilde{q}_k = Av_{k-1} - Q_{k-1} r_k, \quad r_{k,k} = \|\tilde{q}_k\| \quad \text{and} \quad q_k = \tilde{q}_k / r_{k,k}. \quad (28)$$

When $r_{k,k} = 0$ we can simply replace \tilde{q}_k with any vector that is orthogonal to Q_{k-1} [4, 21]. The matrix $R_k^T R_k$ can also be efficiently computed by

$$R_k^T R_k = \begin{pmatrix} R_{k-1}^T & 0 \\ r_k^T & r_{k,k} \end{pmatrix} \begin{pmatrix} R_{k-1} & r_k \\ 0 & r_{k,k} \end{pmatrix} = \begin{pmatrix} R_{k-1}^T R_{k-1} & R_{k-1}^T r_k \\ r_k^T R_{k-1} & r_k^T r_k + r_{k,k}^2 \end{pmatrix}. \quad (29)$$

Up to this point, we have not used any additional structure of the twice continuously differentiable convex function $\Psi(x)$. In general, calculating the gradient $\nabla \Psi(x)$ or

the Hessian $\nabla^2\Psi(x)$ could be quite computationally expensive. For instance, if we consider the example $\Psi(x) = \Psi_p(Lx)$ the smooth approximation of $\frac{1}{p}\|Lx\|_p^p$, evaluating this gradient requires a matrix-vector product with both L and L^T . However, by also saving the tall and skinny matrix $LV_k \in \mathbb{R}^{s \times k}$, we can further reduce the computational cost. Let us consider $\Psi(x) = \tilde{\Psi}(Lx)$ with a matrix $L \in \mathbb{R}^{s \times n}$ and twice continuously differentiable convex function $\tilde{\Psi} : \mathbb{R}^s \rightarrow \mathbb{R}$. There is obviously no loss of generality since we can always take $L = I_n$. Recall that for the ℓ_p norm we take $\tilde{\Psi}(z) = \Psi_p(z)$, while for the general form Tikhonov problem we have $\tilde{\Psi}(z) = \frac{1}{2}\|z\|_2^2$. Further improvements in the latter case will be presented in section 4.4.

In addition to saving the tall and skinny matrices V_k and AV_k we also save the matrix LV_k . We introduce recurrences for $z_k = Lx_k$ and $t_k = Ax_k$, i.e. we get

$$\begin{aligned} z_k &= Lx_k = Lx_{k-1} + \gamma_k L\Delta x_k = z_{k-1} + \gamma_k LV_k \Delta y_k = z_{k-1} + \gamma_k \Delta z_k \\ t_k &= Ax_k = Ax_{k-1} + \gamma_k A\Delta x_k = t_{k-1} + \gamma_k AV_k \Delta y_k = t_{k-1} + \gamma_k \Delta t_k \end{aligned}$$

with $\Delta z_k = (LV_k)\Delta y_k$ and $\Delta t_k = (AV_k)\Delta y_k$ computed as tall and skinny matrix vector products and $z_0 = t_0 = 0$. When we consider the case $L = I_n$ we obviously get the simplification $z_k = x_k$. Forming the Hessian $V_k^T \nabla^2 \Psi(x_{k-1}) V_k$ in the projected Jacobian (17) with $y = \bar{y}_{k-1}$ can be done efficiently, since we have

$$V_k^T \nabla^2 \Psi(x_{k-1}) V_k = (LV_k)^T \nabla^2 \tilde{\Psi}(z_{k-1}) (LV_k).$$

Remember that for our example $\tilde{\Psi}(z) = \Psi_p(z)$ the matrix $\nabla^2 \tilde{\Psi}(z_{k-1})$ is diagonal. To summarize, the linear system (19) to calculate the Projected Newton direction can be rewritten as

$$\begin{pmatrix} \lambda_{k-1} R_k^T R_k + (LV_k)^T \nabla^2 \tilde{\Psi}(z_{k-1}) (LV_k) & R_k^T R_k \bar{y}_{k-1} - d_k \\ (R_k^T R_k \bar{y}_{k-1} - d_k)^T & 0 \end{pmatrix} \begin{pmatrix} \Delta y_k \\ \Delta \lambda_k \end{pmatrix} = - \begin{pmatrix} \lambda_{k-1} (R_k^T R_k \bar{y}_{k-1} - d_k) + (LV_k)^T \nabla \tilde{\Psi}(z_{k-1}) \\ \frac{1}{2} \|t_{k-1} - b\|^2 - \frac{\sigma^2}{2} \end{pmatrix}. \quad (30)$$

4.3. Efficiently performing the backtracking line search

Similarly as before, we now also save the tall and skinny matrix $A^T AV_k \in \mathbb{R}^{n \times k}$ and introduce a recurrence relation for $w_k = A^T Ax_k$. More specifically, we have

$$w_k = A^T Ax_k = A^T Ax_{k-1} + \gamma_k A^T A \Delta x_k = w_{k-1} + \gamma_k \Delta w_k$$

where we compute $\Delta w_k = (A^T AV_k)\Delta y_k$ using a tall and skinny matrix-vector product and initialize $w_0 = 0$. Note that we need to perform only a tall and skinny matrix-vector product with LV_k , AV_k and $A^T AV_k$ and that we then can compute z_k , t_k and w_k for many different values of the step-length γ_k with only vector additions. This is very useful for efficiently performing the backtracking line search. We calculate the gradient

in (12) using only a matrix-vector product with L^T (no matrix-vector product with L anymore), i.e. we have:

$$\nabla \Psi(x_k) = L^T \nabla \tilde{\Psi}(z_k).$$

The above definitions now allow us to efficiently perform the backtracking line search. Indeed, using the definition for t_k, w_k and z_k we can write

$$F(x_k, \lambda_k) = \begin{pmatrix} \lambda_k (w_k - A^T b) + L^T \nabla \tilde{\Psi}(z_k) \\ \frac{1}{2} \|t_k - b\|^2 - \frac{\sigma^2}{2} \end{pmatrix}. \quad (31)$$

Hence, no additional matrix-vector products with A, A^T or L are needed to compute this vector, only one matrix-vector product with L^T each time the step-length is reduced. Note that \tilde{v}_k , as defined in (21), is the first component of this function, so we do not need to perform any additional calculations to obtain this vector. Using the above, we can now formulate the Projected Newton method for solving (11) with $\Psi(x) = \tilde{\Psi}(Lx)$, see algorithm 1. Line 11 has been added in algorithm 1 to make sure the regularization parameter λ_k remains strictly positive.

4.4. Further improvements for general form Tikhonov regularization

If we choose $\Psi(x) = \frac{1}{2} \|Lx\|_2^2$ with $L \in \mathbb{R}^{s \times n}$ (or equivalently $\tilde{\Psi}(z) = \frac{1}{2} \|z\|^2$) we recover the general form Tikhonov problem

$$\min_{x \in \mathbb{R}^n} \frac{1}{2} \|Lx\|_2^2 \quad \text{subject to} \quad \frac{1}{2} \|Ax - b\|_2^2 = \frac{\sigma^2}{2} \quad (32)$$

and algorithm 1 can be improved even further. First we observe that $\nabla \Psi(x) = L^T Lx$ and $\nabla^2 \Psi(x) = L^T L$ (or equivalently $\nabla \tilde{\Psi}(z) = z$ and $\nabla^2 \tilde{\Psi}(z) = I_s$). By considering a reduced QR decomposition of the tall and skinny matrix $LV_k \in \mathbb{R}^{s \times k}$ and also saving the matrix $L^T LV_k \in \mathbb{R}^{n \times k}$ we can reorganize the algorithm in a way, such that we only need a single matrix-vector product with L^T each iteration, instead of one for each time we need to compute $F(x_k, \lambda_k)$ for the backtracking line search. This leads to an improvement when the step-length γ_k has to be reduced multiple times before the sufficient decrease condition is satisfied.

Let $\tilde{Q}_k \in \mathbb{R}^{s \times k}$ with orthonormal columns and $\tilde{R}_k \in \mathbb{R}^{k \times k}$ upper-triangular, such that the reduced QR decomposition of LV_k is given by $LV_k = \tilde{Q}_k \tilde{R}_k$. The Hessian for the regularization term in (30) can be rewritten as

$$(LV_k)^T \nabla^2 \tilde{\Psi}(z_{k-1}) (LV_k) = (LV_k)^T (LV_k) = \tilde{R}_k^T \tilde{R}_k.$$

Similarly we have for the gradient in the right-hand side of (30) the following simplification

$$(LV_k)^T \nabla \tilde{\Psi}(z_{k-1}) = (LV_k)^T Lx_{k-1} = (LV_k)^T LV_k \bar{y}_{k-1} = \tilde{R}_k^T \tilde{R}_k \bar{y}_{k-1}.$$

Algorithm 1 Projected Newton method for $\Psi(x) = \tilde{\Psi}(Lx)$

```

1:  $\bar{y}_0 = 0; z_0 = 0; t_0 = 0; w_0 = 0; \tau = 0.9; c = 10^{-4};$  # Initializations
2:  $AV_0 = A^T AV_0 = LV_0 = \emptyset;$ 
3:  $\tilde{v}_0 = A^T b; d_1 = \|\tilde{v}_0\|; v_0 = \tilde{v}_0/d_1; V_1 = v_0;$  # Matvec with  $A^T$ 
4:  $F_0 = \left(-\lambda_0 \tilde{v}_0^T, \frac{1}{2}\|b\|^2 - \frac{\sigma^2}{2}\right)^T;$  # Compute  $F_0 = F(x_0, \lambda_0)$ 
5: for  $k = 1, 2, \dots$ , until convergence do
6:    $AV_k = [AV_{k-1}, Av_{k-1}]; A^T AV_k = [A^T AV_{k-1}, A^T (Av_{k-1})];$  # Matvec with  $A$  and  $A^T$ 
7:    $LV_k = [LV_{k-1}, Lv_{k-1}];$  # Matvec with  $L$ 
8:   Calculate  $Q_k, R_k$  and  $R_k^T R_k$  by (27)-(29) # QR decomposition  $A$ 
9:   Calculate  $\Delta y_k$  and  $\Delta \lambda_k$  by solving (30) # Projected Newton direction
10:   $\lambda_k = \lambda_{k-1} + \Delta \lambda_k;$ 
11:  if  $\lambda_k > 0$  then  $\gamma_k = 1;$  else  $\gamma_k = -\tau \lambda_{k-1} / \Delta \lambda_k; \lambda_k = \lambda_{k-1} + \gamma_k \Delta \lambda_k;$  end if
12:   $\Delta z_k = (LV_k) \Delta y_k; \Delta t_k = (AV_k) \Delta y_k; \Delta w_k = (A^T AV_k) \Delta y_k;$ 
13:   $(y_k^T, z_k^T, t_k^T, w_k^T) = (\bar{y}_{k-1}^T, z_{k-1}^T, t_{k-1}^T, w_{k-1}^T) + \gamma_k (\Delta y_k^T, \Delta z_k^T, \Delta t_k^T, \Delta w_k^T);$ 
14:   $\tilde{v}_k = \lambda_k (w_k - \tilde{v}_0) + L^T \nabla \tilde{\Psi}(z_k);$  # Matvec with  $L^T$ 
15:   $F_k = \left(\tilde{v}_k^T, \frac{1}{2}\|t_k - b\|^2 - \frac{\sigma^2}{2}\right)^T;$  # Compute  $F_k = F(x_k, \lambda_k)$ 
16:  while  $\frac{1}{2}\|F_k\|^2 \geq (\frac{1}{2} - c\gamma_k)\|F_{k-1}\|^2$  do # Backtracking line search
17:     $\gamma_k = \tau \gamma_k;$ 
18:     $(y_k^T, z_k^T, t_k^T, w_k^T, \lambda_k) = (\bar{y}_{k-1}^T, z_{k-1}^T, t_{k-1}^T, w_{k-1}^T, \lambda_{k-1}) + \gamma_k (\Delta y_k^T, \Delta z_k^T, \Delta t_k^T, \Delta w_k^T, \Delta \lambda_k);$ 
19:     $\tilde{v}_k = \lambda_k (w_k - \tilde{v}_0) + L^T \nabla \tilde{\Psi}(z_k);$  # Matvec with  $L^T$ 
20:     $F_k = \left(\tilde{v}_k^T, \frac{1}{2}\|t_k - b\|^2 - \frac{\sigma^2}{2}\right)^T;$  # Compute  $F_k = F(x_k, \lambda_k)$ 
21:  end while
22:   $\bar{y}_k = (y_k^T, 0)^T; d_{k+1} = (d_k^T, 0)^T;$ 
23:   $v_k = \tilde{v}_k - \sum_{j=0}^{k-1} (v_j^T \tilde{v}_k) v_j;$  # Gram-Schmidt
24:   $v_k = v_k / \|v_k\|; V_{k+1} = [V_k, v_k]$  # Normalize and add new vector to basis
25: end for
26:  $x_k = V_k y_k;$ 

```

When the basis V_k is expanded, we can efficiently update the QR decomposition of LV_k , similarly as in (27) - (29). Next, let us define a new auxiliary vector $u_k = L^T Lx_k$. We again have a recurrence for this variable:

$$u_k = L^T Lx_k = L^T Lx_{k-1} + \gamma_k L^T L \Delta x_k = u_{k-1} + \gamma_k L^T LV_k \Delta y_k = u_{k-1} + \gamma_k \Delta u_k$$

where we compute $\Delta u_k = (L^T LV_k) \Delta y_k$ as a tall and skinny matrix-vector product and initialize $u_0 = 0$. Now we can remove the matrix-vector product with L^T from the backtracking line search. Indeed, we simply replace the term $L^T \nabla \tilde{\Psi}(z_k)$ with u_k , since $\nabla \tilde{\Psi}(z_k) = z_k = Lx_k$. Note that due to these simplifications, there is no need for the auxiliary variable z_k anymore. Hence, we also do not need the tall and skinny matrix-vector product $\Delta z_k = (LV_k) \Delta y_k$ on line 12 in algorithm 1. To summarize, we construct and save the matrix $L^T LV_k$, which requires one matrix-vector product with L^T . We remove the auxiliary variable z_k and add the new variable u_k . We replace the tall and skinny matrix-vector product for Δz_k with $\Delta u_k = (L^T LV_k) \Delta y_k$ on line 12. We replace

the construction of \tilde{v}_k on lines 14 and 19 with

$$\tilde{v}_k = \lambda_k (w_k - \tilde{v}_0) + u_k$$

such that there is no need anymore to compute it using a matrix-vector product with L^T . Lastly, we compute the reduced QR decomposition of LV_k and instead of calculating the Projected Newton direction on line 9 using (30) we now calculate it as

$$\begin{pmatrix} \lambda_{k-1} R_k^T R_k + \tilde{R}_k^T \tilde{R}_k & R_k^T R_k \bar{y}_{k-1} - d_k \\ (R_k^T R_k \bar{y}_{k-1} - d_k)^T & 0 \end{pmatrix} \begin{pmatrix} \Delta y_k \\ \Delta \lambda_k \end{pmatrix} = - \begin{pmatrix} \lambda_{k-1} (R_k^T R_k \bar{y}_{k-1} - d_k) + \tilde{R}_k^T \tilde{R}_k \bar{y}_{k-1} \\ \frac{1}{2} \|t_k - b\|^2 - \frac{\sigma^2}{2} \end{pmatrix}. \quad (33)$$

The dominant cost per iteration of the Projected Newton method for general form Tikhonov regularization is the matrix-vector product with A , A^T , L and L^T . The most important difference with the (more general) implementation given by algorithm 1 is that there is no more matrix-vector product with L^T present in the backtracking line search. See algorithm 4 in the appendix for a detailed description of the method.

Remark 4.3. *It is possible to replace the ℓ_2 norm for the data fidelity term with the ℓ_q norm with $1 \leq q \leq 2$, i.e. to consider the constrained optimization problem*

$$\min_{x \in \mathbb{R}^n} \frac{1}{p} \|Lx\|_p^p \quad \text{subject to} \quad \frac{1}{q} \|Ax - b\|_q^q = \frac{1}{q} \|e\|_q^q. \quad (34)$$

It is straightforward to extend the Projected Newton method such that it can solve (a smooth approximation of) this problem. We can simply take the smooth approximation $\Psi_q(Ax - b)$ of $\frac{1}{q} \|Ax - b\|_q^q$ and consider computational improvements similarly to how we treated $\Psi_p(Lx)$. This leads to an algorithm with dominant cost a matrix-vector product with A , A^T , L and L^T in each iteration and an additional matrix-vector product with A^T and L^T each time the step-length is reduced in the backtracking line search.

5. Reference methods

In this section we describe two reference methods that we will use to compare the Projected Newton method with in section 6. The first one can be used to solve the General Form Tikhonov problem (32), while the second one can be used to obtain an approximate solution for the ℓ_p regularized problem (1).

5.1. Generalized Krylov subspace method

The first method we describe is the Generalized Krylov subspace (GKS) Tikhonov regularization method developed in [4], see algorithm 2. The GKS algorithm can only be used to solve the General Form Tikhonov problem. However, since it served as inspiration for this work and bears resemblance to our approach, we believe it deserves

some attention. It also constructs a Generalized Krylov subspace basis $V_k \in \mathbb{R}^{n \times k}$ for $k \geq l$ (although a different one) and computes the solution to the projected problem

$$y_k = \underset{y \in \mathbb{R}^k}{\operatorname{argmin}} \|AV_k y - b\|_2^2 + \alpha_k \|LV_k y\|_2^2. \quad (35)$$

where α_k is determined such that $\|AV_k y_k - b\| = \sigma$. Note that α_k can be determined using a scalar root-finder, which requires that (35) is solved multiple times. The GKS algorithm starts for $k = l$ with some initial l -dimensional orthonormal basis $V_l \in \mathbb{R}^{n \times l}$, for instance the basis for the Krylov subspace $\mathcal{K}_l(A^T A, A^T b)$, where the dimension l of the initial basis is large enough such that a regularization parameter α_l exists that satisfies the discrepancy principle $\|AV_l y_l - b\| = \sigma$. Subsequently, the basis is expanded by adding the normalized residual of the unreduced problem, i.e.

$$\tilde{v} = (A^T A + \alpha_k L^T L)V_k y_k - A^T b, \quad v_{new} = \tilde{v} / \|\tilde{v}\|. \quad (36)$$

In exact arithmetic this vector is already orthogonal to V_k . However, the authors in [4] suggest to add a reorthogonalization step to enforce orthogonality in the presence of round-off errors. Algorithm 2 can be efficiently implemented such that the dominant cost of a single iteration are four matrix-vector products, namely with A, A^T, L and L^T , same as for algorithm 4. For more details we refer to [4].

Let us briefly comment on the difference between the GKS algorithm and Projected Newton (for general form Tikhonov regularization). While both methods use Generalized Krylov subspaces, the way in which the iterates are calculated is significantly different. While the iterates generated by the Projected Newton method only satisfy the discrepancy principle after a certain number of iterations, the GKS constructs iterates x_k that all satisfy $\|Ax_k - b\| = \sigma$. Moreover, in each iteration of the GKS algorithm, the projected minimization problem is also solved exactly, while the Projected Newton method only performs a single Newton iteration for each dimension k . The basis V_k constructed in algorithm 2 is thus similar to the basis generated in algorithm 4, although not the same since both methods compute different iterates.

Lastly, we briefly mention that the GKS algorithm also closely resembles the Generalized Arnoldi Tikhonov (GAT) method [2]. The latter method uses the Arnoldi algorithm to construct a basis V_k for the Krylov subspace $\mathcal{K}_k(A, b)$, which implies that it can only be applied to square matrices A . In each iteration of the GAT method, (35) is solved for a single value of α_k and then the regularization parameter is updated using a single step of the secant method based on the discrepancy principle. The Krylov subspace basis is subsequently expanded using one step of the Arnoldi algorithm. In contrast to the GKS method, the intermediate iterates x_k in the GAT method do not necessarily need to satisfy discrepancy principle.

5.2. Hybrid iteratively reweighted norm - Projected Newton method

The second reference method we consider is a hybrid method that combines the iteratively reweighted norm (IRN) algorithm [7, 12] with the Projected Newton method

Algorithm 2 The GKS algorithm [4]

-
- 1: Construct initial $V_l \in \mathbb{R}^{n \times l}$ with $\mathcal{R}(V_l) = \mathcal{K}_l(A^T A, A^T b)$ and $V_l^T V_l = I_l$
 - 2: **for** $k = l, l+1, l+2, \dots$, until convergence **do**
 - 3: Calculate α_k and the solution y_k of (35) such that $\|AV_k y_k - b\| = \sigma$.
 - 4: Calculate new basis vector v_{new} by (36) and reorthogonalize.
 - 5: Expand basis $V_{k+1} = [V_k, v_{new}]$.
 - 6: **end for**
 - 7: $x_k = V_k y_k$
-

for Tikhonov regularization. It is able to solve the constrained optimization problem (34) with ℓ_q data fidelity term and ℓ_p regularization term. However, for the sake of presentation we focus our discussion on the simplified case with $q = 2, p = 1$ and $L = I_n$.

The main idea is to replace the non-differentiable term $\|x\|_1$ with a sequence of ℓ_2 norm approximations $\|L_k x\|_2^2$ for $k \geq 0$ with a (diagonal) weighting matrix $L_k \in \mathbb{R}^{n \times n}$. To do so, we first consider the matrix

$$\bar{L}(x) = \text{diag} \left(\frac{1}{\sqrt{|[x]_i|}} \right)_{i=1, \dots, n} \quad (37)$$

where $[x]_i$ is the (non-standard §) notation for the i th component of the vector $x \in \mathbb{R}^n$. Obviously (37) is only well-defined if $[x]_i \neq 0$ for all i . In that case we have

$$\|\bar{L}(x)x\|_2^2 = \sum_{i=1}^n \left(\frac{[x]_i}{\sqrt{|[x]_i|}} \right)^2 = \sum_{i=1}^n \frac{[x]_i^2}{|[x]_i|} = \sum_{i=1}^n |[x]_i| = \|x\|_1.$$

To avoid division by zero, we slightly alter the definition of $\bar{L}(x)$, as follows:

$$\tilde{L}(x) = \text{diag} \left(\frac{1}{\sqrt{\tau([x]_i)}} \right)_{i=1, \dots, n}, \quad \text{with } \tau(t) = \begin{cases} |t| & \text{if } |t| \geq 10^{-6} \\ 10^{-6} & \text{if } |t| < 10^{-6} \end{cases}. \quad (38)$$

The value 10^{-6} is arbitrary and can be replaced by any small constant, but this choice seems to work well in practice. The idea of the hybrid IRN - Projected Newton approach is to solve the sequence of problems

$$x_k = \underset{x \in \mathbb{R}^n}{\text{argmin}} \quad \frac{1}{2} \|L_k x\|_2^2 \quad \text{subject to} \quad \frac{1}{2} \|Ax - b\|_2^2 = \frac{\sigma^2}{2} \quad (39)$$

with $L_k = \tilde{L}(x_{k-1})$ for $k \geq 1$ and $L_0 = I_n$. Since the matrix L_k is diagonal and thus easily invertible we consider a slight reformulation of this problem. In the actual implementation used in the numerical experiments in section 6 we compute the solution of (39) by first transforming it to the standard form Tikhonov problem

$$\hat{x}_k = \underset{\hat{x} \in \mathbb{R}^n}{\text{argmin}} \quad \frac{1}{2} \|\hat{x}\|_2^2 \quad \text{subject to} \quad \frac{1}{2} \|AL_k^{-1} \hat{x} - b\|_2^2 = \frac{\sigma^2}{2}$$

§ To avoid confusion with our notation of x_k as k th iteration of an algorithm.

and solving this problem using the Projected Newton method for standard form Tikhonov regularization [3]. The solution to (39) is now given by $x_k = L_k^{-1} \hat{x}_k$.

Note that we can not simply use the standard IRN algorithm [7] to compare with the Projected Newton method since the former method can only be used to solve

$$\min_{x \in \mathbb{R}^n} \frac{1}{q} \|Ax - b\|_q^q + \frac{\alpha}{p} \|Lx\|_p^p \quad (40)$$

with a fixed regularization parameter. To conclude this section, we like to mention a few other interesting hybrid methods which combine the IRN approach with a projection step on a lower dimensional subspace. In [6, 9] the authors combine the IRN approach with flexible Krylov subspace methods for the ℓ_p regularized problem (1), but it only works for invertible matrices L . In [20] an algorithm that can solve (40) is developed which combines the IRN approach and projection step on a Generalized Krylov subspace. However, the latter method can only be used with a fixed regularization parameter.

Algorithm 3 Hybrid IRN - Projected Newton algorithm

- 1: Compute x_0 the solution of (39) with $L_0 = I_n$
 - 2: **for** $k = 1, 2, \dots$, until convergence **do**
 - 3: Update weighting matrix $L_k = \tilde{L}(x_{k-1})$ defined by (38).
 - 4: Compute x_k the solution of (39) using Projected Newton method.
 - 5: **end for**
-

6. Numerical experiments

In this section we perform a number of experiments to illustrate the behavior of the Projected Newton method and to compare it with Newton's method and the two reference methods described in section 5. We start with some small scale toy models to illustrate different interesting properties and then consider larger, more representative test-problems to study the quality of the obtained solution. We also comment on possible different convergence criteria that can be used. All experiments are performed using MATLAB R2020a with machine precision $\epsilon_{ps} \approx 2.2204 \times 10^{-16}$.

6.1. Generalized Krylov subspaces and induced tridiagonal structure

Experiment 1. We start with a small experiment that justifies calling the basis V_k generated in the Projected Newton method a Generalized Krylov subspace, see (21) and (22) and the discussion following these expressions. We take a small matrix $A \in \mathbb{R}^{200 \times 100}$ with random elements between -1 and 1 and take as exact solution a parabola x_{ex} with components $[x_{ex}]_{i+1} = (-1 + ih)^2$ for $i = 0, \dots, 99$ and $h = 2/99$. Next, we obtain a right-hand side b by adding 1% Gaussian noise to the exact right-hand side $b_{ex} = Ax_{ex}$, which means we have $\|b - b_{ex}\| / \|b_{ex}\| = 0.01$. Moreover, we choose parameters $\lambda_0 = 1$, $\eta = 1$ and stop the algorithm when $\|F(x_k, \lambda_k)\| < 10^{-10}$. We apply the Projected

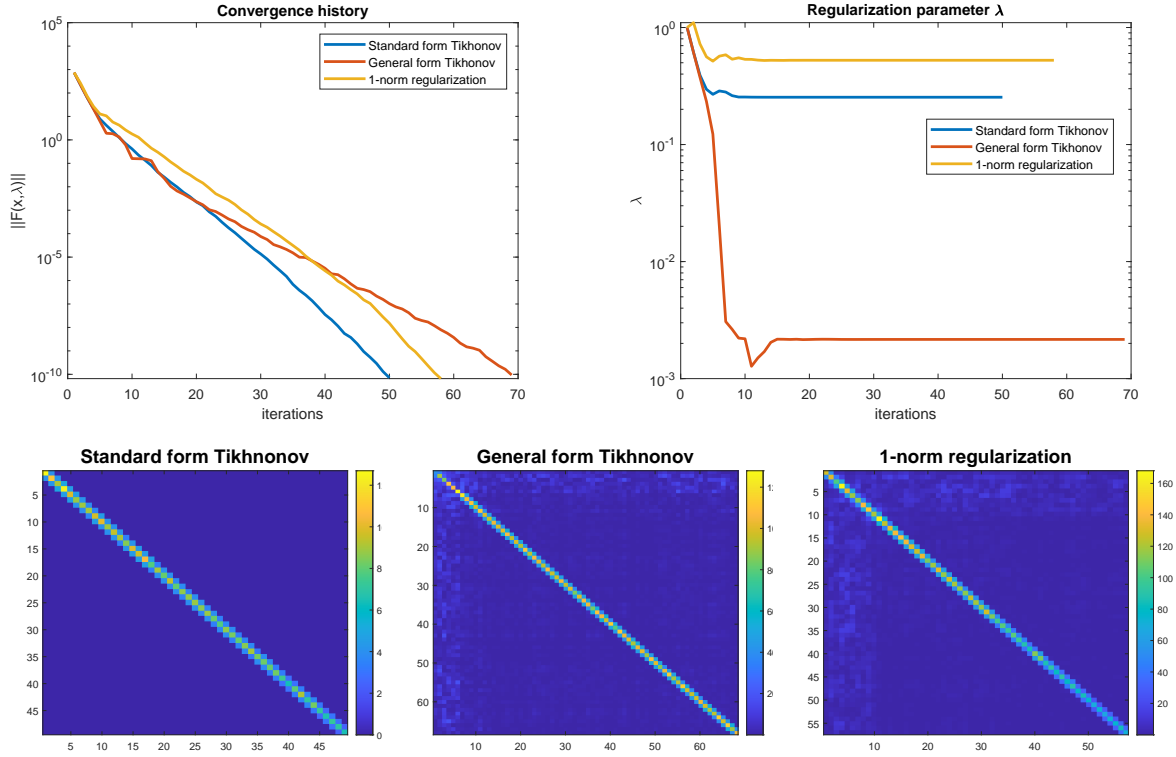


Figure 2: **Experiment 1.** (Top) Convergence history (left) and regularization parameter (right) for standard form Tikhonov, general form Tikhonov and ℓ_1 norm regularization (i.e. $\Psi(x) = \Psi_1(x)$) applied to test-problem with $A \in \mathbb{R}^{200 \times 100}$ randomly generated matrix, exact solution with components $[x_{ex}]_{i+1} = (-1 + ih)^2$ for $i = 0, \dots, 99$ and $h = 2/99$. 1% Gaussian noise is added to the exact right-hand side $b_{ex} = Ax_{ex}$. (Bottom) Tridiagonal structure induced by the Generalized Krylov subspace.

Newton method to the standard form Tikhonov problem, to the general form Tikhonov problem with $L \in \mathbb{R}^{(n-1) \times n}$ the forward finite difference operator given by (3) and the regularized problem with $\Psi(x) = \Psi_1(x)$ as defined in (6), the smooth approximation to the ℓ_1 norm with $\beta = 10^{-4}$.

In figure 2 (top) we plot the convergence history in terms of $\|F(x_k, \lambda_k)\|$ for the three regularized problems and we show that the regularization parameter λ_k stabilizes quickly. Here and in what follows the index k denotes the iteration index. As explained in section 4.1, we know that the basis V_k generated by the Projected Newton method for the standard form Tikhonov problem is in fact a Krylov subspace basis due to the shift-invariance property of Krylov subspaces (24). As a consequence we have that $V_k^T(A^T A + \alpha_k I)V_k$ with $\alpha_k = 1/\lambda_k$ is a tridiagonal matrix. In figure 2 (bottom) we have illustrated this by showing the absolute value of the elements of this matrix for the final iteration k . Similarly for the general form Tikhonov problem we show the matrix $V_k^T(A^T A + \alpha_k L^T L)V_k$ and for the ℓ_1 regularized problem we show $V_k^T(A^T A + \alpha_k \nabla^2 \Psi_1(x_k))V_k$ (each with their respective basis V_k and parameter α_k). For

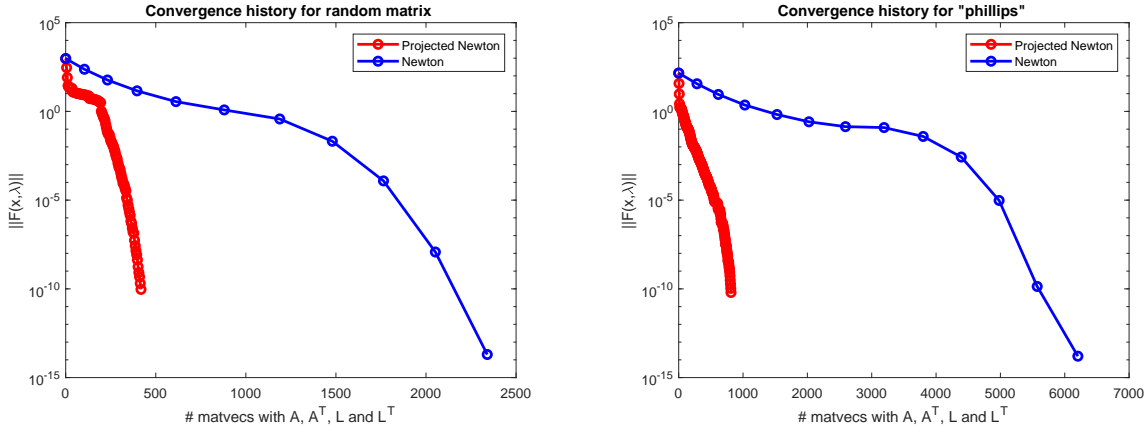


Figure 3: **Experiment 2.** Comparison of convergence history of Projected Newton method and Newton's method in terms of number of matrix-vector products for $\Psi(x) = \Psi_1(Lx)$ with $L \in \mathbb{R}^{(n-1) \times n}$ the finite difference operator given by (3).

the latter two problems, this matrix is not really tridiagonal since V_k is not an actual Krylov subspace, but due to the rapid stabilization of the regularization parameter, we can observe that the size of the elements on the three main diagonals is much larger than the size of the other elements. This shows that the matrix V_k does closely resemble an actual Krylov subspace basis in this particular case. We do not claim that this is a representative test-problem since a random matrix A is in general not ill-conditioned, however it does illustrate the point we want to make. The effect may of course be less pronounced for other, more realistic test-problems.

6.2. Comparison with Newton's method and GKS

Experiment 2. We compare the Projected Newton method with Newton's method applied to the nonlinear system of equations $F(x, \lambda) = 0$, see (12). We use the Krylov subspace method MINRES to compute the Newton direction $\Delta_N = J(x, \lambda)^{-1}F(x, \lambda)$ in a matrix free fashion. We put the maximum number of iteration of MINRES equal to 200 and take a relative tolerance of 10^{-6} as stopping criteria. We use the same backtracking line search as in algorithm 1 to ensure global convergence.

We consider two different linear inverse problems, namely the same test-problem as in the previous experiment, i.e. a randomly generated matrix A with a parabola as exact solution and the more realistic test-problem `phillips` from the MATLAB package Regularization Tools [22] with $n = 200$, which gives a matrix $A \in \mathbb{R}^{200 \times 200}$ with condition number $\kappa(A) \approx 10^7$. The MATLAB function `phillips` also provides an exact solution x_{ex} and corresponding exact right-hand side b_{ex} . For both test-problems we add 1% Gaussian noise and apply the Projected Newton method to the ℓ_1 regularized problem with $L \in \mathbb{R}^{(n-1) \times n}$ the finite difference operator given by (3), i.e. we choose $\Psi(x) = \Psi_1(Lx)$. The other parameters are kept the same as before.

In figure 3 we plot $\|F(x_k, \lambda_k)\|$ for both algorithms in function of the number of

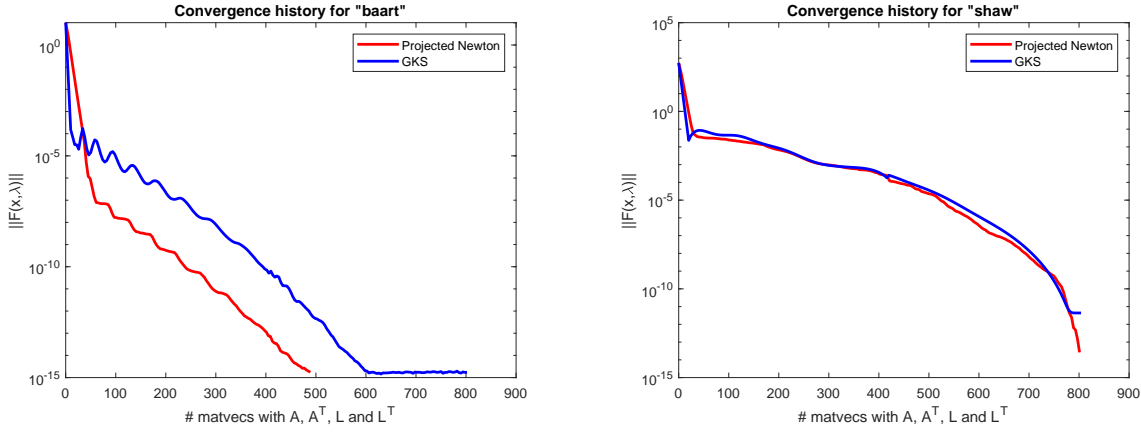


Figure 4: **Experiment 3.** Comparison of convergence history of Projected Newton method and the Generalized Krylov subspace method algorithm 2 in terms of number of matrix-vector products for general form Tikhonov problem with $L \in \mathbb{R}^{(n-1) \times n}$ the finite difference operator given by (3).

matrix-vector products with A , A^T , L and L^T . Each iteration of MINRES to compute the Newton direction Δ_N requires a matrix-vector product with A , A^T , L and L^T to apply the Jacobian matrix to a vector. Note that every iteration of Newton's method requires multiple MINRES iteration. In addition, we also need to perform these 4 matrix-vector products to evaluate $F(x, \lambda)$, which becomes computationally expensive if the step-length is reduced many times in the backtracking line search. Recall that the Projected Newton method has to perform a matrix-vector product with A , A^T , L and L^T in each iteration and an additional matrix-vector product with L^T each time the step-length is reduced. The left figure shows the result for the test-problem with random matrix A , where the quadratic local convergence of Newton's method can clearly be observed. Hence, the number of (outer) iterations for Newton's method is quite low. However, the total number of matrix-vector products is much larger than for the Projected Newton method due to the large cost per Newton iteration. The effect becomes even worse for the ill-conditioned test-problem **phillips**, for which the result is shown in the right figure. Although convergence of Newton's method is very fast in terms of (outer) iterations, the number of matrix-vector products needed for each iteration is quite large. The benefit of using the Projected Newton method over Newton's method is apparent from these examples.

Experiment 3. In the next experiment we compare the Projected Newton method with the GKS algorithm, see algorithm 2. To do so, we consider the general form Tikhonov problem and again take $L \in \mathbb{R}^{(n-1) \times n}$ the finite difference operator (3) and test-problems **baart** and **shaw** from the Regularization Tools package, which gives us two matrices $A \in \mathbb{R}^{200 \times 200}$ that both have a condition number $\kappa(A) \approx 10^{19}$. The other parameters are kept the same as above. The dominant cost for both the GKS

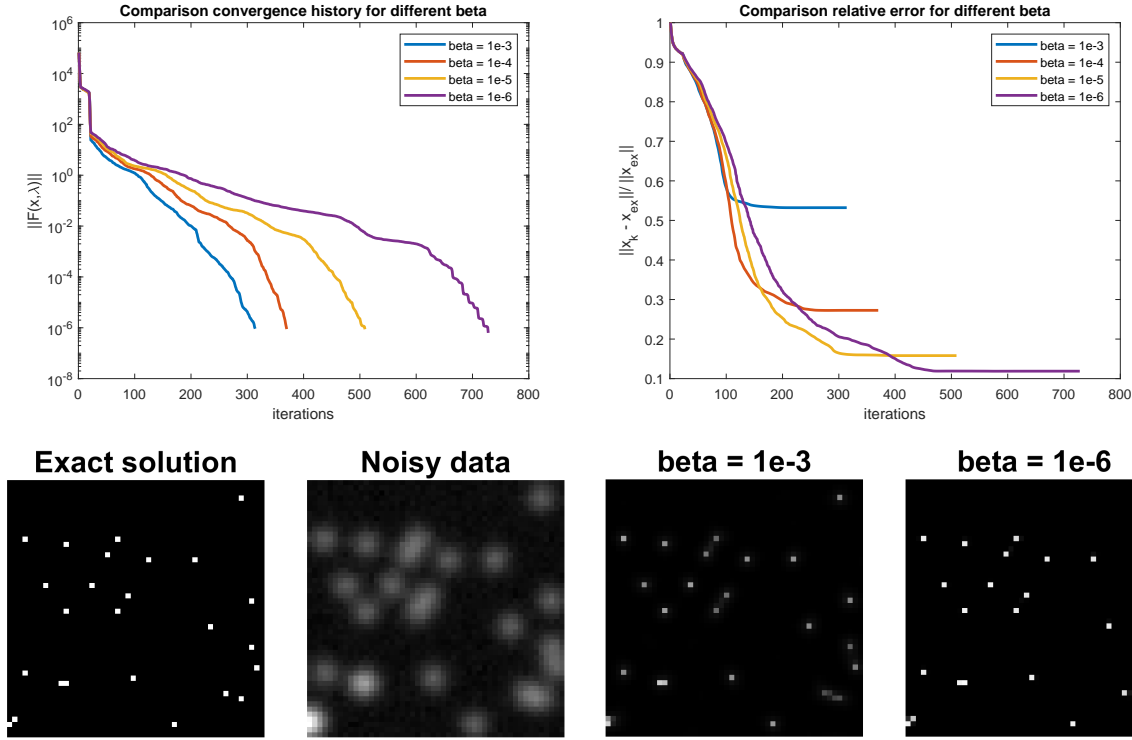


Figure 5: **Experiment 4.** (Top) Comparison of convergence history (left) and relative error (right) for different values of the smoothing parameter β for an image deblurring problem with $\Psi(x) = \Psi_1(x)$. (Bottom) Exact solution and noisy data for deblurring experiment. Reconstructed solutions for $\beta = 10^{-3}$ and $\beta = 10^{-6}$ are also shown.

algorithm and Projected Newton method are the matrix-vector products with A, A^T, L and L^T in each iteration. Recall that we removed the need to perform an additional matrix-vector product with L^T in the backtracking line search in the case of general form Tikhonov regularization by the improvements presented in section 4.4. The result is given by figure 4. The convergence history for both methods is quite similar, which is not that surprising since both methods look for a solution in a very similar Generalized Krylov subspace. Although the Projected Newton method slightly outperforms the GKS method for test-problem `baart`, the benefit is modest. For the `shaw` test-problem convergence is almost entirely the same. However, this experiment does nicely illustrate that the true strength of the Projected Newton method lies in its generality. Although the Projected Newton method can be applied to a more general regularization problem, its performance is comparable to a state-of-the-art algorithm specifically designed for general form Tikhonov regularization.

6.3. Sparse reconstruction

In the previous experiments we have not yet looked at the quality of the obtained solution and how well the smooth function $\Psi_p(x)$ actually approximates $\frac{1}{p} \|x\|_p^p$. In this

section we study these questions for test-problems with a sparse exact solution, such that the (approximate) ℓ_1 regularized solution, i.e. with $\Psi(x) = \Psi_1(x)$, should give a good reconstruction.

Experiment 4. As a first example we take a small sparse image $X \in \mathbb{R}^{50 \times 50}$ with approximately 10% of the pixels set to one. We take the deblurring matrix $A \in \mathbb{R}^{2500 \times 2500}$ provided by the function `PRblurgauss` from the IR Tools MATLAB package [23] (with optional parameter *blurlevel* set to *mild*). The exact solution x_{ex} is obtained by stacking all columns X and we get the corresponding exact data $b_{ex} = Ax_{ex}$. We add 1% Gaussian noise to the data. See figure 5 for an illustration of the exact solution and noisy data. To study the quality of the reconstruction we consider different values of β used in the definition of the smooth approximation $\Psi_1(x)$, more precisely we take $\beta = 10^{-3}, 10^{-4}, 10^{-5}$ and 10^{-6} . The smaller this value, the closer $\Psi_1(x)$ is to the actual ℓ_1 norm. We take $\lambda_0 = 10^5$ and stop the algorithm when $\|F(x_k, \lambda_k)\| < 10^{-6}$. The result of this experiment is given by figure 5. In the top left figure we show the value $\|F(x_k, \lambda_k)\|$ for the different choices of β . We can observe that convergence is slower when β is smaller. This is not entirely surprising since a small value of β also implies that $\Psi_1(x)$ becomes less smooth and that the condition number of the Hessian $\nabla^2 \Psi_1(x)$ can become larger, see (8). However, a smaller value of β also gives a better reconstruction, as shown by the relative error in the right figure. In figure 5 we also show the actual reconstruction for $\beta = 10^{-3}$ and $\beta = 10^{-6}$. It is clear that the latter image is indeed a better reconstruction since in that case $\Psi_1(x)$ is a better approximation of $\|x\|_1$. When choosing this value, one should try to find a balance between improved quality of the reconstruction and the amount of work needed to find the solution. Lastly, we would also like to point out the stable behavior of the error on the top right plot of figure 5 and the fact that the error has stabilized well before a very accurate solution has been found (in terms of $\|F(x_k, \lambda_k)\|$). We explore this last observation in a bit more detail in section 6.4.

Experiment 5. For the next experiment we compare the Projected Newton method with algorithm 3 based on the Iteratively reweighted norm approach. The tolerance of the sub-problems on lines 1 and 4 of algorithm 3 is set to 10^{-6} . We apply both algorithms to the deblurring test-problem above with $\beta = 10^{-6}$. In addition to the deblurring problem, we also consider an example from Computed Tomography (CT). We take an exact sparse image $X \in \mathbb{R}^{128 \times 128}$ with approximately 10% of the pixels set to one. We generate the matrix A that represents a two-dimensional parallel beam geometry with 180 angles between 0 and π and with 128 detectors using the ASTRA toolbox [24]. This results in a matrix of size $23,040 \times 16,384$. The noisy data is generated as before with 1% Gaussian noise and we set $\beta = 10^{-6}$ and $\lambda_0 = 1$. In figure 6 we show the result of this experiment for the deblurring test-problem (left) and CT test-problem (right), where we plot the relative error for both algorithms in terms of the number of matrix-vector products with A and A^T . It is clear that the Projected Newton method significantly

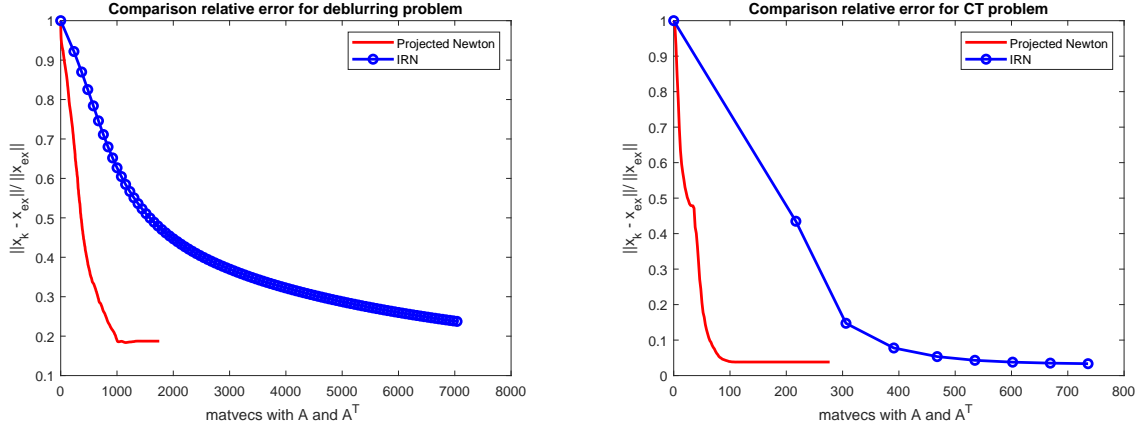


Figure 6: **Experiment 5.** Comparison of hybrid IRN - Projected Newton method (algorithm 3) and Projected Newton method for sparse reconstruction with $\Psi(x) = \Psi_1(x)$.

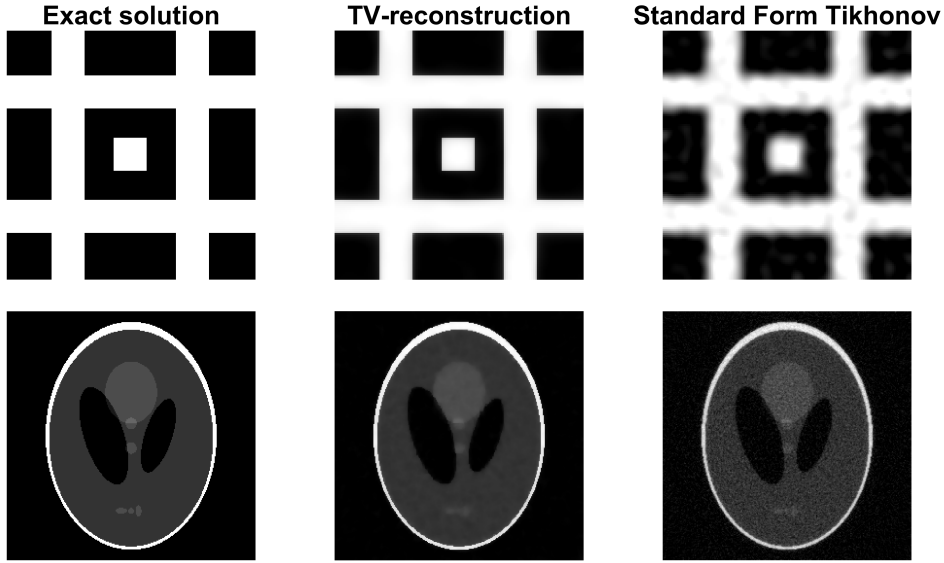


Figure 7: **Experiment 6.** The exact and reconstructed solutions for the image deblurring test-problem (top) and CT test-problem (bottom), as well as the solution obtained by standard form Tikhonov regularization as a reference.

outperforms the IRN approach for both test-problems and that both methods produce solution of similar quality (as measured by the relative error).

6.4. Total variation regularization

Experiment 6. For our final numerical experiment we consider total variation regularization, i.e. we choose $\Psi(x) = \Psi_1(Lx)$ the smooth approximation of $\text{TV}(x)$, see (2), with L defined as (4). With this experiment we want to compare different

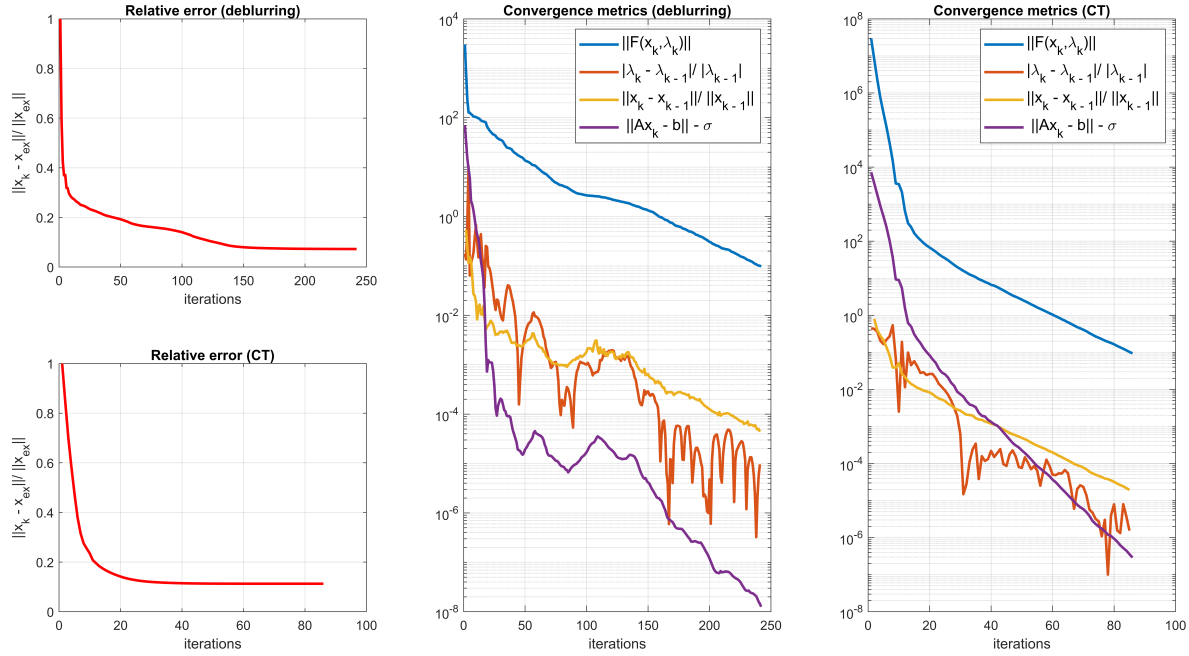


Figure 8: **Experiment 6.** The relative error and other (computable) convergence metrics are shown for the deblurring and CT test-problem with $\Psi(x) = \Psi_1(Lx)$ the smooth approximation of anisotropic total-variation function, where L is defined as (4).

convergence metrics that can possibly be used to formulate a stopping criteria. We already observed in the previous experiment that it is definitely possible that the relative error stabilizes well before $\|F(x_k, \lambda_k)\|$ is very small.

We again take an example from image deblurring with matrix A generated by the MATLAB function `PRblurgauss` from the IR Tools package and a CT example with matrix generated using the ASTRA Toolbox. For the deblurring test-problem we take the exact image $X \in \mathbb{R}^{128 \times 128}$ as shown in figure 7 (top) and add 1% Gaussian noise to the data. The corresponding deblurring matrix has size $16,384 \times 16,384$ and the regularization matrix has size $32,512 \times 16,384$. For the CT test-problem we take the well-known modified shepp-logan phantom of size 256×256 as exact solution, see figure 7 (bottom). We again use a two-dimensional parallel beam geometry, but now taking 180 angles and 256 detectors, leading to an underdetermined matrix A of size $46,080 \times 65,536$ and regularization matrix of size $130,560 \times 65,536$. Next, we add 0.5% Gaussian noise to the data.

We stop the algorithm when $\|F(x_k, \lambda_k)\| < 10^{-1}$, set $\beta = 10^{-4}$ and show the reconstructed solution for both test-problems in figure 7 as well as the solution obtained by standard form Tikhonov regularization as a reference. Next, we show the relative error in figure 8, as well as the following four convergence metrics:

- (i) the norm of the nonlinear equation evaluated in the iterates: $\|F(x_k, \lambda_k)\|$,
- (ii) the relative difference of the regularization parameter: $|\lambda_k - \lambda_{k-1}|/|\lambda_{k-1}|$,

- (iii) the relative difference of the solution: $\|x_k - x_{k-1}\|/\|x_{k-1}\|$,
- (iv) the mismatch with the discrepancy principle: $\|Ax_k - b\| - \sigma$.

All these values can be computed during the iterations without a noticeable computational overhead. Note that it follows from lemma 4.2 that the value used in (iv) is positive. The values $\|F(x_k, \lambda_k)\|$ form a decreasing sequence since we enforce this by the backtracking line search. Hence this convergence metric behaves quite nice and smooth. However, the relative error stagnates well before this value becomes very small. Hence, it seems that it is not necessary to find the actual root of $F(x, \lambda)$ to obtain a good solution to the inverse problem. The relative difference of the regularization parameter decreases much more rapidly, but has also a severely non-monotonic behavior and can exhibit large spikes. The relative difference in the solution x_k seems to be a bit more smooth, although also definitely not monotonic. The mismatch with the discrepancy principle is the value that seems to decrease the most rapidly for these test-problems among all the convergence metrics we have shown. Moreover, it is also smoother than the metrics (ii) and (iii). What this indicates is that (for these particular test-problems) the Projected Newton method converges quickly to a solution x_k that (approximately) satisfies the discrepancy principle, while it takes much longer to actually satisfy the optimality condition (10). However, it seems that it is not that important for the quality of the reconstruction by observing the relative error. Due to these reasons we suggest to use (iv) as the convergence criteria. Lastly we mention the very rapid convergence of the Projected Newton method in terms of the relative error. For the deblurring test-problem the relative error stabilizes around iteration $k = 150 \ll n = 16,384$, while for the CT test-problem it stabilizes around iteration $k = 30 \ll n = 65,536$.

7. Conclusions

We present a new and efficient Newton-type algorithm to compute (an approximation of) the solution of the ℓ_p regularized linear inverse problem with a general, possibly non-square or non-invertible regularization matrix. Simultaneously it determines the corresponding regularization parameter such that the discrepancy principle is satisfied. First, we describe a convex twice continuously differentiable approximation of the ℓ_p norm for $p \geq 1$. We then use this approximation to formulate a constrained optimization problem that describes the problem of interest. In iteration k of the algorithm we project this optimization problem on a Generalized Krylov subspace basis of dimension k . We show that the Newton direction of this projected problem results in a descent direction for the original problem, which we use in a backtracking line search. We show how to efficiently implement this strategy, mainly using the reduced QR decomposition of a tall and skinny matrix. Further improvements in the case of general form Tikhonov regularization are presented as well.

Next, we illustrate the interesting structure of Generalized Krylov subspaces and compare the efficiency of the Projected Newton method with other state-of-the-art approaches with a number of numerical experiments. We show that the Projected

Newton method is able to produce a highly accurate solution to an ill-posed linear inverse problem with a modest computational cost. Furthermore, we show that we are successfully able to produce sparse solutions with the approximation of the ℓ_1 norm and that the approximation of the total variation regularization function also performs well. Lastly, we comment on a number of different convergence criteria that can be used and argue that the mismatch with the discrepancy principle is a suitable candidate.

Appendix A. Pseudocode for general form Tikhonov regularization

In this section we present the pseudocode for the Projected Newton method applied to the general form Tikhonov problem, i.e. algorithm 1 with $\Psi(x) = \frac{1}{2}||Lx||_2^2$. The computational improvements from section 4.4 are applied.

Algorithm 4 Projected Newton method for general form Tikhonov regularization

```

1:  $\bar{y}_0 = 0; u_0 = 0; t_0 = 0; w_0 = 0; \tau = 0.9; c = 10^{-4};$  # Initializations
2:  $AV_0 = A^T AV_0 = LV_0 = L^T LV_0 = \emptyset;$ 
3:  $\tilde{v}_0 = A^T b; d_1 = ||\tilde{v}_0||; v_0 = \tilde{v}_0/d_1; V_1 = v_0;$  # Matvec with  $A^T$ 
4:  $F_0 = \left(-\lambda_0 \tilde{v}_0^T, \frac{1}{2}||b||^2 - \frac{\sigma^2}{2}\right)^T;$  # Compute  $F_0 = F(x_0, \lambda_0)$ 
5: for  $k = 1, 2, \dots$ , until convergence do
6:    $AV_k = [AV_{k-1}, Av_{k-1}]; A^T AV_k = [A^T AV_{k-1}, A^T(Av_{k-1})];$  # Matvec with  $A$  and  $A^T$ 
7:    $LV_k = [LV_{k-1}, Lv_{k-1}]; L^T LV_k = [L^T LV_{k-1}, L^T(Lv_{k-1})];$  # Matvec with  $L$  and  $L^T$ 
8:   Calculate  $Q_k, R_k$  and  $R_k^T R_k$  by (27)-(29) # QR decomposition  $A$ 
9:   Calculate  $\tilde{Q}_k, \tilde{R}_k$  and  $\tilde{R}_k^T \tilde{R}_k$  (similarly) # QR decomposition  $L$ 
10:  Calculate  $\Delta y_k$  and  $\Delta \lambda_k$  by solving (33) # Projected Newton direction
11:   $\lambda_k = \lambda_{k-1} + \Delta \lambda_k;$ 
12:  if  $\lambda_k > 0$  then  $\gamma_k = 1;$  else  $\gamma_k = -\tau \lambda_{k-1} / \Delta \lambda_k;$   $\lambda_k = \lambda_{k-1} + \gamma_k \Delta \lambda_k;$  end if
13:   $\Delta u_k = (L^T LV_k) \Delta y_k; \Delta t_k = (AV_k) \Delta y_k; \Delta w_k = (A^T AV_k) \Delta y_k;$ 
14:   $(y_k^T, u_k^T, t_k^T, w_k^T) = (\bar{y}_{k-1}^T, u_{k-1}^T, t_{k-1}^T, w_{k-1}^T) + \gamma_k (\Delta y_k^T, \Delta u_k^T, \Delta t_k^T, \Delta w_k^T);$ 
15:   $\tilde{v}_k = \lambda_k (w_k - \tilde{v}_0) + u_k;$ 
16:   $F_k = \left(\tilde{v}_k^T, \frac{1}{2}||t_k - b||^2 - \frac{\sigma^2}{2}\right)^T;$  # Compute  $F_k = F(x_k, \lambda_k)$ 
17:  while  $\frac{1}{2}||F_k||^2 \geq (\frac{1}{2} - c\gamma_k)||F_{k-1}||^2$  do # Backtracking line search
18:     $\gamma_k = \tau \gamma_k;$ 
19:     $(y_k^T, u_k^T, t_k^T, w_k^T, \lambda_k) = (\bar{y}_{k-1}^T, u_{k-1}^T, t_{k-1}^T, w_{k-1}^T, \lambda_{k-1}) + \gamma_k (\Delta y_k^T, \Delta u_k^T, \Delta t_k^T, \Delta w_k^T, \Delta \lambda_k);$ 
20:     $\tilde{v}_k = \lambda_k (w_k - \tilde{v}_0) + u_k;$ 
21:     $F_k = \left(\tilde{v}_k^T, \frac{1}{2}||t_k - b||^2 - \frac{\sigma^2}{2}\right)^T;$  # Compute  $F_k = F(x_k, \lambda_k)$ 
22:  end while
23:   $\bar{y}_k = (y_k^T, 0)^T; d_{k+1} = (d_k^T, 0)^T;$ 
24:   $v_k = \tilde{v}_k - \sum_{j=0}^{k-1} (v_j^T \tilde{v}_k) v_j;$  # Gram-Schmidt
25:   $v_k = v_k / ||v_k||; V_{k+1} = [V_k, v_k]$  # Normalize and add new vector to basis
26: end for
27:  $x_k = V_k y_k;$ 

```

References

- [1] Per Christian Hansen. *Discrete Inverse Problems*. Society for Industrial and Applied Mathematics, 2010.
- [2] Silvia Gazzola and Paolo Novati. Automatic parameter setting for Arnoldi-Tikhonov methods. *Journal of Computational and Applied Mathematics*, 256:180 – 195, 2014.
- [3] Jeffrey Cornelis, Nick Schenkels, and Wim Vanroose. Projected Newton method for noise constrained Tikhonov regularization. *Inverse Problems*, 36(5), mar 2020.
- [4] Jorg Lampe, Lothar Reichel, and Heinrich Voss. Large-scale Tikhonov regularization via reduction by orthogonal projection. *Linear Algebra and its Applications*, 436(8):2845 – 2865, 2012.
- [5] D. Calvetti, S. Morigi, L. Reichel, and F. Sgallari. Tikhonov regularization and the L-curve for large discrete ill-posed problems. *Journal of Computational and Applied Mathematics*, 123(1):423 – 446, 2000. Numerical Analysis 2000. Vol. III: Linear Algebra.
- [6] Silvia Gazzola and James G. Nagy. Generalized Arnoldi-Tikhonov method for sparse reconstruction. *SIAM Journal on Scientific Computing*, 36(2):B225–B247, 2014.
- [7] Paul Rodriguez and Brendt Wohlberg. An efficient algorithm for sparse representations with ℓ_p data fidelity term. In *Proceedings of 4th IEEE Andean Technical Conference (ANDESCON)*, 2008.
- [8] Scott Shaobing Chen, David L. Donoho, and Michael A. Saunders. Atomic decomposition by Basis Pursuit. *SIAM J. Sci. Comput.*, 20(1):3361, December 1998.
- [9] Julianne Chung and Silvia Gazzola. Flexible Krylov methods for ℓ_p regularization. *SIAM Journal on Scientific Computing*, 41(5):S149–S171, 2019.
- [10] I. F. Gorodnitsky and B. D. Rao. Sparse signal reconstruction from limited data using FOCUSS: a re-weighted minimum norm algorithm. *IEEE Transactions on Signal Processing*, 45(3):600–616, 1997.
- [11] T Chan, Selim Esedoglu, Frederick Park, and A Yip. Total variation image restoration: Overview and recent developments. In *Handbook of mathematical models in computer vision*, pages 17–31. Springer, 2006.
- [12] B. Wohlberg and P. Rodriguez. An Iteratively Reweighted norm algorithm for minimization of Total Variation functionals. *IEEE Signal Processing Letters*, 14(12):948–951, Dec 2007.
- [13] Jorge Nocedal and Stephen Wright. *Numerical optimization*. Springer Science & Business Media, 2006.
- [14] Germana Landi. The Lagrange method for the regularization of discrete ill-posed problems. *Computational Optimization and Applications*, 39(3):347–368, 2008.
- [15] Adil Bagirov, Napsu Karimtsa, and Marko M Mäkelä. *Introduction to Nonsmooth Optimization: theory, practice and software*. Springer, 2014.
- [16] C. C. Paige and M. A. Saunders. Solution of sparse indefinite systems of linear equations. *SIAM Journal on Numerical Analysis*, 12(4):617–629, 1975.
- [17] Christopher C Paige and Michael A Saunders. LSQR: An algorithm for sparse linear equations and sparse least squares. *ACM Transactions on Mathematical Software (TOMS)*, 8(1):43–71, 1982.
- [18] Gene Golub and William Kahan. Calculating the singular values and pseudo-inverse of a matrix. *Journal of the Society for Industrial and Applied Mathematics, Series B: Numerical Analysis*, 2(2):205–224, 1965.
- [19] Stephen Boyd, Stephen P Boyd, and Lieven Vandenberghe. *Convex optimization*. Cambridge university press, 2004.
- [20] A. Lanza, S. Morigi, L. Reichel, and F. Sgallari. A Generalized Krylov Subspace Method for ℓ_p - ℓ_q Minimization. *SIAM Journal on Scientific Computing*, 37(5):S30–S50, 2015.
- [21] James W Daniel, Walter Bill Gragg, Linda Kaufman, and Gilbert W Stewart. Reorthogonalization and stable algorithms for updating the gram-schmidt QR factorization. *Mathematics of Computation*, 30(136):772–795, 1976.

- [22] Per Christian Hansen. Regularization tools: a Matlab package for analysis and solution of discrete ill-posed problems. *Numerical algorithms*, 6(1):1–35, 1994.
- [23] Silvia Gazzola, Per Christian Hansen, and James G Nagy. IR tools: a MATLAB package of iterative regularization methods and large-scale test problems. *Numerical Algorithms*, 81(3):773–811, 2019.
- [24] Wim Van Aarle, Willem Jan Palenstijn, Jan De Beenhouwer, Thomas Altantzis, Sara Bals, K Joost Batenburg, and Jan Sijbers. The ASTRA toolbox: A platform for advanced algorithm development in electron tomography. *Ultramicroscopy*, 157:35–47, 2015.